

Lawrence Berkeley National Laboratory

Recent Work

Title

THERMAL PULSING OF METALS UHDER HIGH PRESSUEE

Permalink

<https://escholarship.org/uc/item/9dd3n8n1>

Author

Stark, Walter Alfred

Publication Date

1967-04-01

University of California
Ernest O. Lawrence
Radiation Laboratory

THERMAL PULSING OF METALS UNDER HIGH PRESSURE

TWO-WEEK LOAN COPY

*This is a Library Circulating Copy
which may be borrowed for two weeks.
For a personal retention copy, call
Tech. Info. Division, Ext. 5545*

DISCLAIMER

This document was prepared as an account of work sponsored by the United States Government. While this document is believed to contain correct information, neither the United States Government nor any agency thereof, nor the Regents of the University of California, nor any of their employees, makes any warranty, express or implied, or assumes any legal responsibility for the accuracy, completeness, or usefulness of any information, apparatus, product, or process disclosed, or represents that its use would not infringe privately owned rights. Reference herein to any specific commercial product, process, or service by its trade name, trademark, manufacturer, or otherwise, does not necessarily constitute or imply its endorsement, recommendation, or favoring by the United States Government or any agency thereof, or the Regents of the University of California. The views and opinions of authors expressed herein do not necessarily state or reflect those of the United States Government or any agency thereof or the Regents of the University of California.

UCRL-17454

UNIVERSITY OF CALIFORNIA
Lawrence Radiation Laboratory
Berkeley, California
AEC Contract No. W-7405-eng-48

THERMAL PULSING OF METALS UNDER HIGH PRESSURE

Walter Alfred Stark, Jr.

(Ph. D. Thesis)

April 1967

TABLE OF CONTENTS

ABSTRACT	
INTRODUCTION	1
PART I. HEAT CAPACITY MEASUREMENTS.	7
Experimental	19
Results	37
Conclusions	57
PART II. THERMAL SHOCKING	61
Results	68
Conclusions	70
APPENDIX I	72
APPENDIX II	79
APPENDIX III	81
TABLES	82
ACKNOWLEDGEMENTS	86
REFERENCES	87

-v-

THERMAL PULSING OF METALS UNDER HIGH PRESSURE

Walter Alfred Stark, Jr.

Inorganic Materials Research Division, Lawrence Radiation Laboratory,
Department of Chemistry,
University of California, Berkeley, California

ABSTRACT

April 1967

The theory and instrumentation of a method for measuring the heat capacities of metals and semiconductors as functions of temperature and pressure in the Bridgman opposed anvil apparatus are described. The technique involves measurement of the rate of temperature increase in the sample as electrical energy is added at a known rate for a short period of time. The method was used to follow the heat capacity anomaly near the Curie temperature T_c for gadolinium at pressures up to 20 kb; dT_c/dP was found to be $-1.3^\circ\text{K}/\text{kb}$. The heat capacity of iron was measured over the temperature range $150^\circ - 300^\circ\text{K}$ for pressures between 20 and 100 kb; within the experimental uncertainty of 5-6% no variation of the heat capacity with pressure was observed in this interval. Some limitations of the present setup are discussed.

A variation of the above technique using larger current pulses to thermally shock a metal under pressure has been applied to the high pressure transformations of bismuth, tin, and iron. This method appears to yield thermodynamic values of transition pressures and the following fixed points were obtained: bismuth, 81 ± 4 kb; tin, 99 ± 4 kb; and iron, 118 ± 6 kb.

Finally, the dependence of the electrical resistance of iron on the three-halves power of the absolute temperature at pressures greater than 20 kb is noted.

INTRODUCTION

It has often been pointed out that the application of pressure to a solid is one method of decreasing the lattice parameter or interatomic distance; thus properties such as the electrical resistance which depend on the lattice parameter can be conveniently varied for study. Often the techniques required are straightforward adaptations of existing one atmosphere pressure methods, such as, resistance measurement. However, other properties require new, and unfortunately in many cases, less precise, approaches.

The heat capacity of solids, in particular of metals, is one such property which depends on the interatomic distance; of the several components of the heat capacity at constant pressure, C_p , the lattice contribution at constant volume, C_v^l , the electronic heat capacity, C^e , and a dilation heat capacity, $C^d = C_p - C_v$, are all functions of the interatomic spacing. C_v^l is basically related to the force constants between neighboring nuclei, and the electronic heat capacity is dependent upon the shape of the Fermi surface. Both the force constants and the Fermi surface contours are highly dependent on the lattice parameter. The thermal expansion coefficient, α , the isothermal compressibility, χ , and the volume V , are likewise functions of pressure which make up C^d . For other components of the heat capacity of some metals, there is expectation of pressure dependence, as in the case of magnetic order-disorder phenomena.

The classical methods of determining heat capacities by measuring the temperature rise associated with the input of a known amount of energy face dismal prospects for success when applied to metals under pressure, particularly at pressures greater than about 10 kb ($1 \text{ kb} = 10^9 \text{ dynes/cm}^2 = 986.9 \text{ atm} = 1.0196 \cdot 10^3 \text{ kg/cm}^2$). The difficulty is the fact that the

pressure transmitting medium is in intimate contact with the sample and so provides an extremely large path for heat leak from the sample. The mass of the pressure generating apparatus is commonly hundreds to tens of thousands times larger than the sample under study; attempts to see 10% changes in a sample heat capacity would require a precision of perhaps 1 part in 10^5 in a Bridgman opposed anvil setup of the type used in these laboratories.

These problems notwithstanding, there are in the literature records of attempts at measuring heat capacities under pressure, with varying degrees of success. In his 1946 review article, Bridgman¹ comments on several heat capacity determinations of gases to around 2 kb, on work of some of the ammonium halides,² and of solid CH_4 and solid CD_4 ,³ at pressures below 5 kb. In a later review,⁴ he discusses heat capacity calculations for liquids, for which changes in the heat capacity with pressure may be found from the thermal expansion coefficient using the thermodynamic relation:

$$\left(\frac{\partial C_p}{\partial P} \right)_T = -T \left(\frac{\partial^2 V}{\partial T^2} \right)_P \quad (\text{II})$$

where T is the absolute temperature, V is the specific volume, and P is the pressure. Bridgman concludes in the same book that the effect of pressure on the heat capacity of solids is small.

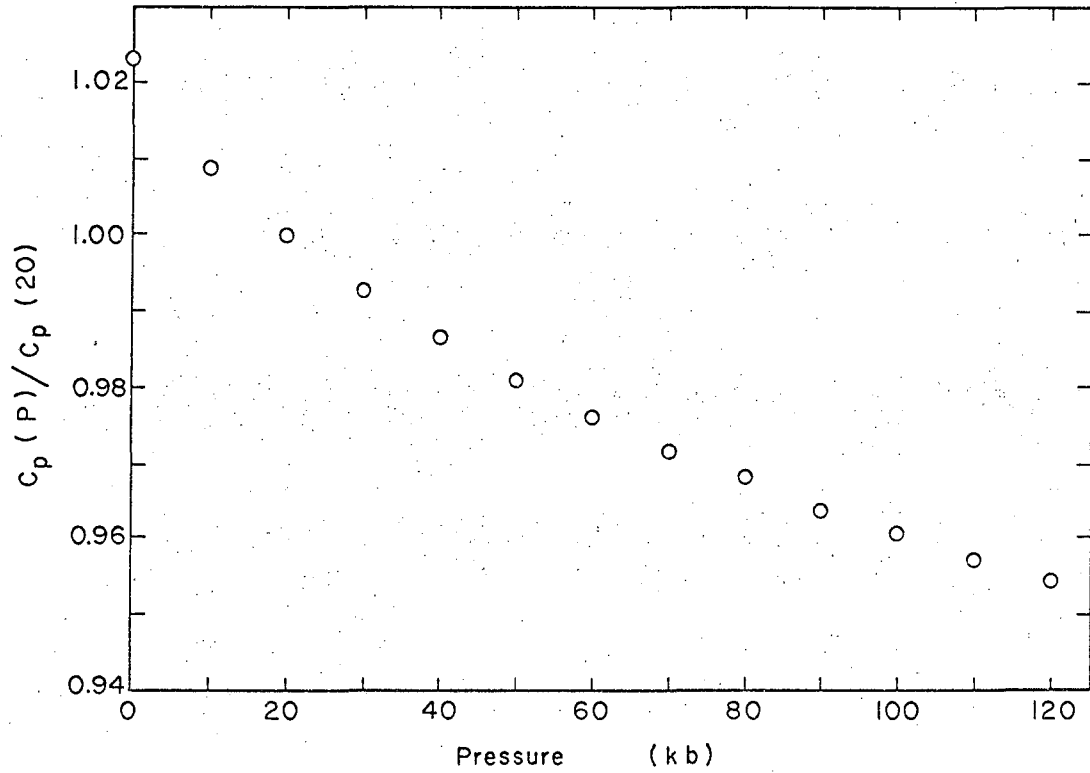
Some direct calorimetry has been done on solids up to pressures of about 10 kb; these investigations include work on solid He,^{5,6} solid H_2 ,⁷ and more recently, on uranium⁸ and cerium.⁹ The studies were performed at temperatures sufficiently low that the heat capacity of the pressure bomb was a determinable, and often small, fraction of the total heat

capacity. The method places unfortunate limitations on both the temperature and pressure ranges, but does retain the precision of good calorimetry.

Equations of state are often goals of high pressure experimenters, and given such an equation, one could calculate C_p in a Debye-Gruneisen approximation. An excellent example is Raimondi's¹⁰ equation of state determination for aluminum. Measurement of the electrical resistance dependence on pressure and temperature allowed determination of a Debye characteristic temperature as a function of pressure. The heat capacity may be calculated and the results are shown in Fig. 1. The technique is straightforward and has given apparently excellent results; however its basic assumptions require nearly free electrons, and resistance due to simple electron-phonon scattering only. A majority of the metals do not fill these requirements and the method presumably would fail.

Other methods have yielded data which in principle allows calculation of heat capacities or changes in heat capacities. Dynamic application of pressure in shock wave work yields equations of state.¹¹⁻¹⁵ It is commonly assumed in these analyses that C_v is constant, and perhaps a second order correction is necessary to calculate C_v , thus determining to what degree the assumption is valid. The pressures attained in shock work can be as high as megabars, and only rarely extends below hundreds of kilobars; it is consequently difficult to relate any changes to zero pressure values. Sometimes, as in the case of iron, one of the metals studied in the present work, there is a phase transition at elevated pressures, and continuity in the heat capacity relative to lower pressures is lost.

One final method should be mentioned. As Pound and Rebka,¹⁶ and Preston, Hanna, and Heberle¹⁷ have shown, measurement of the temperature



XBL 672-938

Fig. 1 Relative heat capacity of Al as a function of pressure (Raimondi¹⁰).

dependence of the absorption intensity in Mössbauer spectroscopy allows determination of a Debye-like temperature characteristic of the host lattice; given this one may compute heat capacities in the Debye approximation. A number of experiments involving the Mössbauer effect under high pressure have been performed¹⁸⁻²² which show the method is feasible. In fact, one paper on tin metal gives the Debye θ as a function of pressure.²² The method is limited by the availability of suitable γ sources; one cannot estimate the effect on the host lattice of an impurity emitter and consequently the emitter and host must be the same element. Only a few convenient sources are available, including Fe⁵⁷, Sn¹¹⁹, and Dy¹⁶¹.

From the foregoing, it is seen that a gap exists in the pressure-temperature region where heat capacity measurements on metals have been carried out. Specifically, for moderate pressures of 10-100 kb and temperatures in the range above 50°K, little work has been done except for a few special cases. The present work describes the development of a general method of measuring the heat capacity of metals in the above mentioned pressure-temperature range. Theoretically the method may also be applied to semiconductors.

The method evolved as a pulsing technique in which the temperature rise, measured as an electrical resistance increase, is continuously monitored while electrical energy is added at a known rate, in a manner somewhat similar to the Wallace, Sidles, and Danielson experiment.²³ Extrapolation back to zero time is required to eliminate the effect of heat conduction from the sample. As will be shown later, the resultant equation gives the heat capacity at constant pressure in terms of the power input, the temperature derivative of the electrical resistance, and the rate of increase of the resistance.

Given the stable and sensitive Tektronix Type W differential comparator amplifier, the apparatus was developed to essentially its present form. Several initial experiments investigated the ferromagnetic-paramagnetic transition of gadolinium. With an eye toward development of an equation of state, work then proceeded to iron and aluminum. The former was chosen for its convenient resistance, compressibility, and Debye temperature; the latter to allow comparison with known data.

While the final setup awaited the development of suitable oscilloscope amplifiers, earlier experiments took advantage of favorable phase diagrams of bismuth, iron, and tin to investigate the effect of momentary heating on the transition pressures of certain phase transformations; the apparent results were transition pressures likely to be closer to the "true" thermodynamic pressure than those measured under more static, isothermal conditions.

PART I. HEAT CAPACITY MEASUREMENTS

The heat capacity of a substance reflects the ability of the constituent particles of the substance to take up in their motions the potential and kinetic energy changes accompanying a rise in temperature. In particular, for a solid metal one commonly has a heat capacity C_V^1 due to the vibrations of the lattice nuclei, and a heat capacity C^e due to the motion of the electrons near the Fermi surface. For metals having d and f electrons, one may also encounter various magnetic heat capacities.

These heat capacities are both pressure and temperature dependent and a proper discussion of these aspects requires a brief review of the origins of heat capacity. More details may be found in standard texts such as Kittel,²⁴ Ziman,²⁵ or Born and Huang.²⁶ The review article of de Launay is also quite informative.

The lattice heat capacity at constant volume has been explained, with good success, by associating energy with the vibrational motions of the nuclei in the regular crystal lattice. Classically it was assumed that each mode of vibration could take up energy $k_B T$, where k_B is Boltzmann's constant, 1.38×10^{-16} erg/deg, and T is the absolute temperature. For one mole of nuclei, each with 3 degrees of vibrational freedom, this meant an energy of $3N_0 k_B T = 3RT$, and consequently a heat capacity $C = \partial E / \partial T = 3R$. While this result gave some theoretical justification for the law of Dulong-Petit, it was far too simple and did not explain those solids which had lower heat capacities. The advent of the concept of discrete energy states and the accessibility to those states provided further explanation.

Earlier workers treated the harmonic oscillator of frequency ν by assuming discrete states characterized by energies

$$E_n = h\nu (n + 1/2) \quad (T1)$$

n being an integer and h Planck's constant. Accessibility to each state is given by the Boltzmann distribution law, so that the average energy \bar{E} of an oscillator is given by

$$\begin{aligned} \bar{E}_{\text{osc}} &= \frac{\sum_{n=0}^{\infty} nh\nu \left(e^{-nh\nu/k_B T} \right)}{\sum_{n=0}^{\infty} e^{-nh\nu/k_B T}} \\ &= \frac{h\nu}{\left(e^{h\nu/k_B T} - 1 \right)} \end{aligned} \quad (\text{T2})$$

neglecting the zero point energy. The heat capacity follows as

$$C = \frac{\partial \bar{E}_{\text{osc}}}{\partial T} = k_B \left(\frac{h\nu}{k_B T} \right)^2 \frac{e^{h\nu/k_B T}}{\left(e^{h\nu/k_B T} - 1 \right)^2} \quad (\text{T3})$$

A crystal lattice is treated as a collection of coupled harmonic oscillators, the frequencies of which are the frequencies of the normal mode vibrations of the crystal system. The energy, and hence the heat capacity, of the lattice is obtained as the sum of the energies Eq. (T2) of all the oscillators:

$$E_{\text{lat}} = \sum_i \frac{h\nu_i}{\left(e^{h\nu_i/k_B T} - 1 \right)} \cdot g(\nu_i) \quad (\text{T4})$$

Here $g(\nu_i)$ is a density function giving the number g of nuclei oscillating at ν_i .

Generally, as shown by Born and von Kármán,²⁸ among others, the distribution of modes in a real lattice is a rather complicated function of

frequency and depends on the nature and relative value of the force constants between neighboring nuclei, next neighbors, and further neighbors. In principle one could take into account the various interactions between all nuclei (and electrons; see the de Launay review) in the crystal lattice, and calculate the distribution function; practically, however, because of the large number ($\sim 3N_0$ /mole) of normal modes, sampling techniques must be used and only an approximation to the distribution curve may be found, as for example, the work on the fcc lattice by Garland and Jura.²⁹

Other theoretical successes in regard to the heat capacity were obtained with different approximations to the distribution function. Einstein assumed a "spike" distribution function with partial success, while Debye treated the collection of nuclei as a continuous medium, and evaluated the density of modes in that approximation. After correction for lattice expansion and the electronic heat capacity, experimental data agreed quite well with Debye theory. The Debye approximation is widely used today and is a partial basis for the present work.

The Debye model, like the Einstein approximation, yields one parameter relations for the energy and entropy of a regular lattice. The energy E is given by

$$E = \int_0^{\omega_{\max}} (\hbar\omega) \left(\frac{3\omega^2}{2\pi^2 v_0^3} \right) d\omega \quad (T5)$$

where \hbar = Planck's constant over 2π ,

$$\omega = 2\pi\nu,$$

v_0 = the velocity of propagation of the oscillation through the lattice.

(A slight approximation has been made here: the transverse and longitudinal velocities are assumed identical.)

ω_{\max} = cut off frequency, defined by

$$\int_0^{\omega_{\max}} g(\omega) d\omega = 3N$$

limiting the total number of modes to $3N$.

The right term in parenthesis in Eq. (T5) represents the distribution function for a 3 dimensional solid continuum while $h\omega$ is the energy of a given vibration. The equation is more commonly written as

$$E = 9RT \left(\frac{T}{\theta_D} \right)^3 \int_0^{\theta_D/T} \frac{u^3 du}{e^u - 1} \quad (T7)$$

where u = dummy variable

θ_D = adjustable parameter

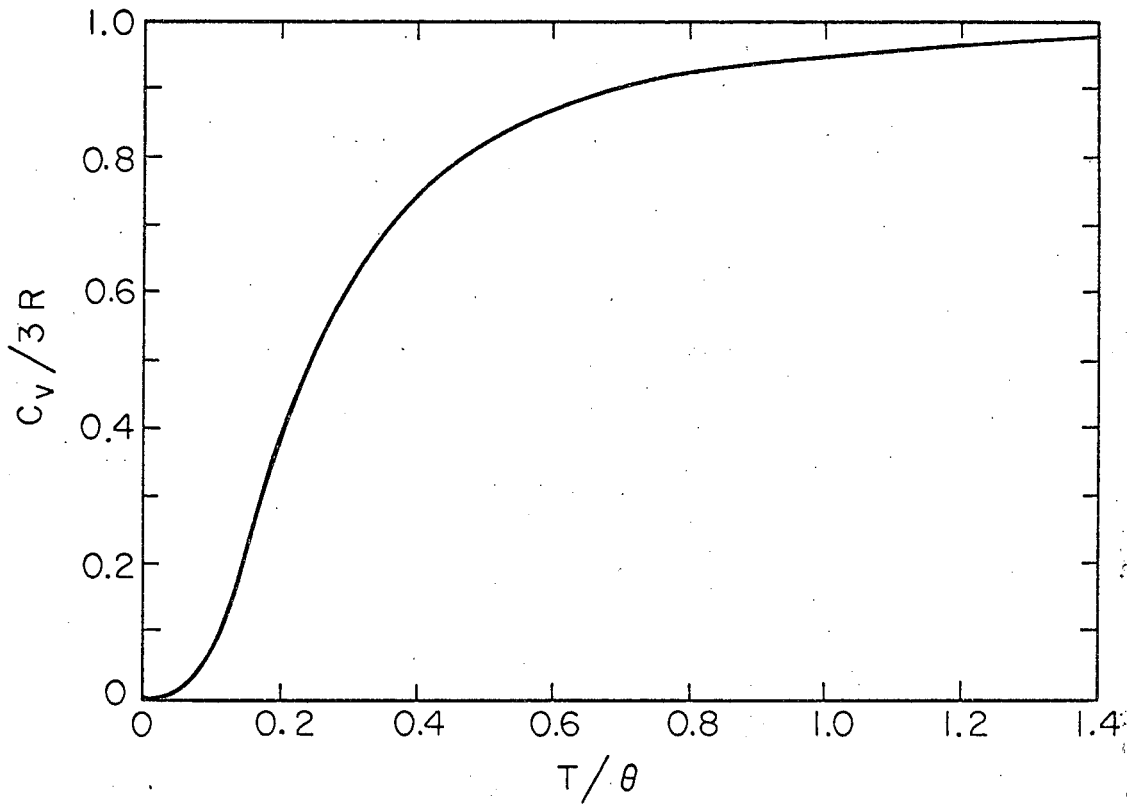
θ_D arises in the theory as the temperature equivalent to the energy of the mode vibrating at the maximum allowed frequency; i.e.,

$$k_B \theta_D = h \nu_{\max} \quad (T8)$$

For metals θ_D is typically of the order 3×10^2 K. The heat capacity follows on differentiation of Eq. (T7) as

$$C_V^1 = 9R \left(\frac{T}{\theta} \right)^3 \int_0^{\theta_D/T} \frac{u^4 e^u du}{(e^u - 1)^2} \quad (T9)$$

This function, as well as the Debye functions for E , S , and A are known and tabulated, for instance, in UCRL Report 17225.³⁰ For convenience in later discussion the Debye C_V^1 curve as a function of T/θ_D is shown in Fig. 2.



XBL672-939

Fig. 2 The Debye lattice heat capacity.

The Debye theory gives C_V^1 as a function of T/θ ; commonly the measured quantity is a total heat capacity at constant pressure, C_p , which has a lattice component C_p^1 . The difference $C_p^1 - C_V^1$, is found from thermodynamics to be³⁴

$$C_p^1 - C_V^1 = \frac{\alpha^2 VT}{\chi} \quad (T13)$$

where α = coefficient of thermal expansion

$$= \frac{1}{V} \left(\frac{\partial V}{\partial T} \right)_P$$

χ = isothermal compressibility

$$= -\frac{1}{V} \left(\frac{\partial V}{\partial P} \right)_T$$

This difference is the "dilation" term, and essentially is the temperature derivative of the energy required to expand the lattice against an external pressure. In the temperature range of the experiments reported later, this term represents approximately 1 - 2% of the total lattice heat capacity.

Another component of the total heat capacity is the electronic heat capacity C^e . This heat capacity arises from those electrons near enough the Fermi surface that they may be excited thermally to take up energy. Only a small fraction of the total number of electrons may do this, giving, as shown in ref. 24, the relation

$$C^e = \left(\frac{\pi^2}{3} \mathcal{D}(\epsilon_F) k_B^2 \right) T \quad (T14)$$

where $\mathcal{D}(\epsilon_F)$ is the density of electronic states at the Fermi surface, with energy = ϵ_F . For a free electron gas; it may be shown²⁴ that

$$C^e = \frac{\pi^2}{2} \frac{Nk_B^2}{\epsilon_F} T = \gamma_e T \quad (T15)$$

It is seen that C^e is inversely proportional to ϵ_F . The simple particle-in-a-box model of a nearly free electron in a metal predicts that the energy levels should rise as the width of the box is decreased, i.e., as the metal is compressed, the energy states of the electrons, and therefore the Fermi level, go up. Thus one expects on the basis of free electron theory that C^e will decrease with increasing pressure. Support for this view comes from some preliminary work of Burton and Jura³⁵ on positron annihilation in aluminum under pressure. It was found that the Fermi momentum increased with pressure roughly as $(V_0/V)^{1/3}$, a result in good agreement with free electron theory. One may also calculate the change with volume assuming that the data of Swenson and co-workers^{36,37} are representative of all metals. From their work on tantalum and mercury one may say that $\partial \ln \gamma_e / \partial \ln V \sim 5$. Realizing the crude nature of this assumption, one may calculate the decrease in γ_e (the derivative is positive, hence γ_e decreases with increasing pressure);

$$\begin{aligned} \Delta \log \gamma_e &\approx \frac{\partial \log \gamma_e}{\partial \log V} \Delta \log V \\ &\sim 5 \cdot \Delta \log V \\ &\sim 5 \cdot (-.023) \\ &\sim -.115 \end{aligned}$$

The change in $\log V$ at $P = 100$ kb has been calculated from the compressibility data given for iron (see Appendix II). γ_e is given as 11.9×10^{-4} cal/deg² mole³⁸ so that $\log \gamma_e = -2.925$. Thus at 100 kb γ_e has decreased

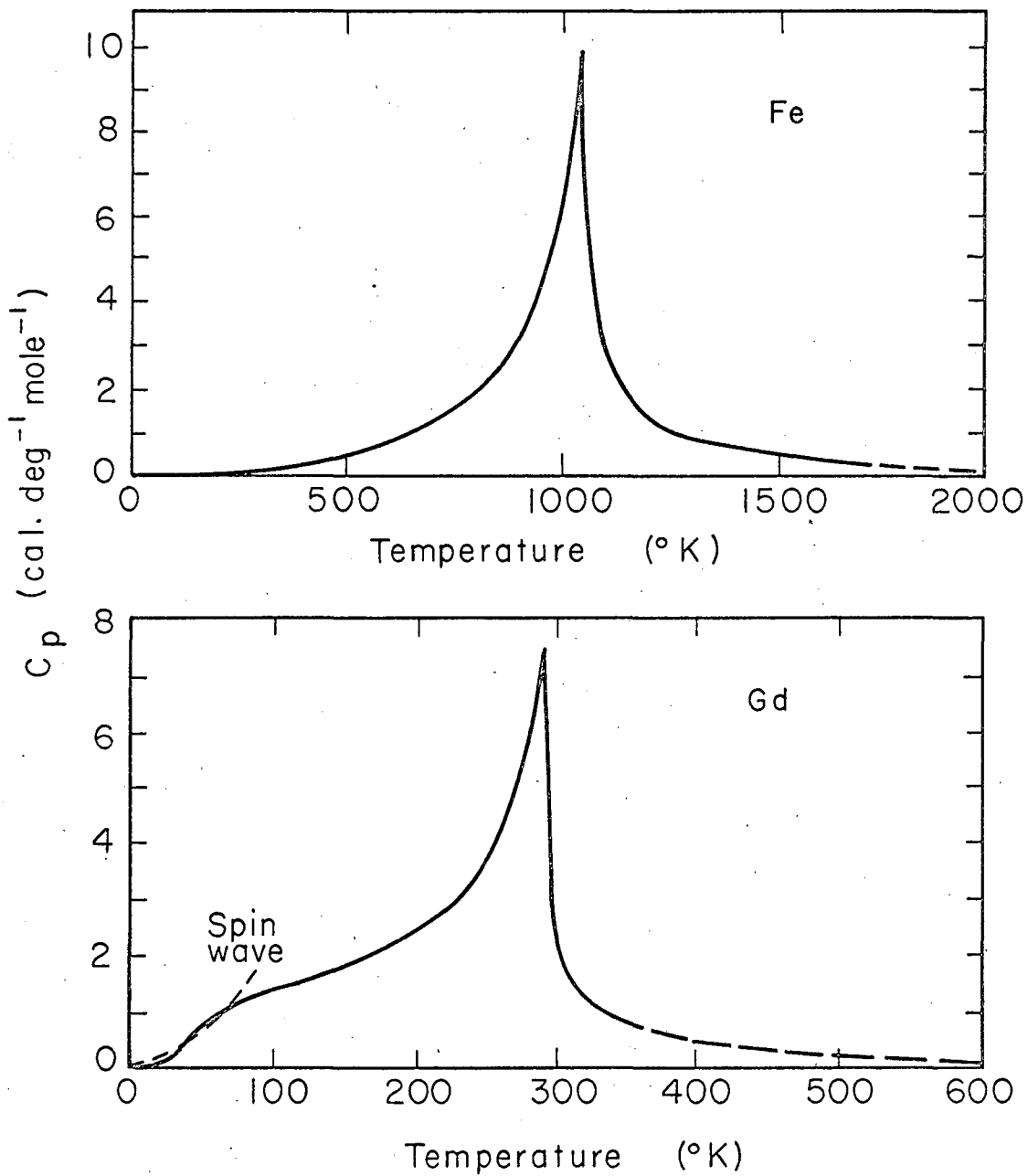
by 25% to $.9 \times 10^{-3}$. Since at room temperature the electronic heat capacity of iron is 6% of the total, a change of 25% in γ_e means a change of 1-2% in the total heat capacity.

Two of the metals in the present study were gadolinium and iron, both of which are ferromagnetic in all or part of the temperature range investigated. There is associated with magnetic properties a heat capacity due to the disorder-order state of the electrons in the $3d$ or $4f$ bands. Hofmann, et al. have discussed the problem at some length.³⁹ They separated the magnetic heat capacity by subtracting the lattice and electronic contributions from the measured C_p , and requiring the magnetic entropy as calculated from the magnetic heat capacity to be $R \ln (2S + 1)$ where S is the spin of the metal. The results for iron and gadolinium at atmospheric pressure are shown in Fig. 3. For iron at room temperature and zero pressure, the magnetic heat capacity is about 2% of the total.

The effect of pressure on the magnetic heat capacity is not known to any great extent; thermodynamically it can be shown¹⁹ that for a second order transition (i.e., a phase transition with no volume or entropy discontinuities) the requirement that the free energy G across the phase boundary be continuous leads to the result

$$\frac{dT_c}{dP} = \frac{TV\Delta\alpha}{\Delta C_p} = \frac{\Delta\alpha}{\Delta X} \quad (T16)$$

$\Delta\alpha$ is the magnitude of the discontinuity in the thermal expansion coefficient, ΔX is the magnitude of the discontinuity in the isothermal compressibility, and ΔC_p is the discontinuity in the heat capacity, all measured across the phase boundary. (Whether or not Eq. (T16) is wholly applicable to the ferromagnetic-paramagnetic transition is a moot point. The Weiss molecular field model yields a second order phase transition,



XBL672-940

Fig. 3 The separated magnetic heat capacities of Fe and Gd (Hofmann, et al.³⁹).

but the experimental behaviour of iron is more complicated, and indicative of a higher order transition. See Pippard,^{39a} Chapter 9). For simple molecular field theory, it is found²⁴ that the exchange integral J is proportional to T_c , the Curie temperature, at which the metal passes from the ferromagnetic state to the paramagnetic state:

$$J = 3k_B T_c / 2z_n S(S + 1) \quad (T17)$$

z_n is the number of neighbor atoms, generally approximated by the number of nearest neighbors. In this same approximation C^{mag} is found to be⁴⁰

$$C^{\text{mag}} = \text{const} \left(\frac{T}{2JS} \right)^{3/2} = A \left(\frac{T}{T_c} \right)^{3/2} \quad (T18)$$

The magnetic heat capacity will follow approximately the change in T_c . Measurements of dT_c/dP for iron⁴¹ and gadolinium^{19, 41-44} give values of ~ 0 and $\sim -1.5^\circ\text{K/kb}$, respectively. The measurements on iron were made only at pressures up to 7 kb, but calculations based on internal field measurements from Mössbauer spectroscopy give essentially the same result, showing a decrease of approximately 2°K at 100 kb.⁴⁵

Given experiments in which the lower limit of the temperature range is sufficiently low to allow determination of the lattice and electronic heat capacities separately from the magnetic ordering heat capacity, it would be possible to measure both the magnetic energy and entropy as a function of pressure. Unfortunately this is not the case in the present experiment; as a matter of fact, high pressure experiments at temperatures below $\sim 60^\circ\text{K}$ have only recently met with success.⁴⁶ The experiments reported here on gadolinium were essentially an early test of the apparatus.

Experimental

The working equation for the experiments on Gd, Fe, and Al was developed as follows: consider a metal sample of resistance R and heat capacity C_p carrying constant current I since time = 0. The energy flow balance is given by

$$\begin{aligned} \frac{dH}{dt} &= \text{Heat flow in} - \text{Heat flow out} \\ &= I^2 R - f(T-T_a) \end{aligned} \quad (E1)$$

The function $f(T-T_a)$ is a cooling function which we have assumed is primarily dependent on the difference between the temperature T of the sample and the temperature T_a of the surroundings. dH/dt represents the rate of increase of the enthalpy of the sample, which is assumed to be at constant pressure. We assume that the electrical resistance at constant pressure is a function of the temperature only

$$\begin{aligned} R &= R(T) \\ \frac{dR}{dT} &= R'(T) \end{aligned} \quad (E2)$$

Under this assumption, and using the relations $E = I R$, where E is the voltage across the sample, and $C_p = (\partial H/\partial T)_p$, one finds

$$\begin{aligned} \frac{dH}{dt} &= C_p \frac{dT}{dt} = C_p \frac{dT}{dR} \cdot \frac{dR}{dt} \\ &= \frac{C_p}{R'} \cdot \frac{1}{I} \cdot \frac{dE}{dt} \end{aligned}$$

and

$$\frac{dE}{dt} = \frac{IR'}{C_p} \left[I^2 R - f(T-T_a) \right] \quad (E3)$$

If one now assumes that the data allow extrapolation back to 0 time where $T = T_a$ and the cooling term vanishes, it is found that

$$\frac{dE}{dt} = \frac{I^3 RR'}{C_p} \quad (E4)$$

which on rearrangement gives

$$C_p = \frac{I^3 RR'}{dE/dt} \quad (E5)$$

Equation (E4) predicts that $dE/dt)_{t=0}$ will be linear in I^3 , a prediction which is verified experimentally to within 3% for iron. Equation (E4) also indicates that 0 current should give $dE/dt = 0$; instead it was found experimentally that the dE/dt intercept was commonly negative, and often could not be explained on the basis of data scatter. In addition, particularly in the case of aluminum, it was found that sometimes $dE/dt \propto I^n$ with n greater than 3.0. This behavior is consistent with heat leakage away from the sample, and it was felt that an analysis taking heat leak into account should be made. The approximation made was the assumption of linear heat transfer at the boundary between the metal sample and the pressure transmitting medium. This "radiation" boundary condition states that the heat flux across a boundary is proportional to the temperature difference across the boundary.⁴⁷

Under this approximation, Eq. (E1) becomes

$$\frac{dH}{dt} = I^2 R - \Delta(T - T_a) \quad (E6)$$

where Δ is the constant of proportionality. Now, in order to make the equation somewhat more tractable one makes the additional assumptions that over the short (2 - 20°K) temperature range involved, C_p is constant

and the resistance R is a linear function of temperature:

$$R = R_a + \beta\tau, \quad \tau = T - T_a ;$$

with these approximations Eq. (E6) may be rewritten as

$$\frac{dH}{dt} = \frac{C_p}{IR'} \quad \frac{dE}{dt} = I^2 R - \frac{\Delta}{\beta} (R - R_a)$$

$$\frac{dE}{dt} = \frac{IR'}{C_p} \left[I^2 R - \frac{\Delta}{\beta} (R - R_a) \right] \quad (E7)$$

One may approximate Δ by going to the steady state, at which

$$\frac{dE}{dt} = 0 = I_{ss}^2 R_{ss} - \frac{\Delta}{\beta} (R_{ss} - R_a)$$

or

$$\Delta = \frac{\beta I_{ss}^2 R_{ss}}{R_{ss} - R_a} \quad (E8)$$

Here the ss subscript represents the values of the variables at the steady state. (In reality this is really only a pseudo steady state, since the medium surrounding the sample is heating slightly, thus changing T_a .)

Substitution of Eq. (E8) into Eq. (E7) yields

$$\frac{dE}{dt} = \frac{IR'}{C_p} \left[I^2 R - I^2 R_{ss} \left(\frac{R - R_a}{R_{ss} - R_a} \right) \right] \quad (E9)$$

The ss subscript has been removed from the I^2 term since $R_{ss} = R_{ss}(I)$.

Now

$$\frac{dE}{dt} = \frac{I^3 R'}{C_p} \left[R - R_{ss} \left(\frac{R - R_a}{R_{ss} - R_a} \right) \right]$$

and

$$\frac{dE}{dt} = \frac{I^2 R_a R'}{C_p} \left[\frac{R_{ss} - R}{R_{ss} - R_a} \right] \quad (E10)$$

or, in terms of observed voltages,

$$\frac{dE}{dt} = \frac{I^2 R'}{C_p} E_a \left[\frac{E_{ss} - E}{E_{ss} - E_a} \right] \quad (E11)$$

A change in variable and integration yields

$$\ln \left[\frac{E_{ss} - E}{E_{ss} - E_a} \right] = - \left(\frac{I^2 R'}{C_p} \frac{E_a}{E_{ss} - E_a} \right) t \quad (E12)$$

The integration constant was evaluated by the boundary condition $E = E_a$ at $t = 0$. If now $\ln[E_{ss} - E/E_{ss} - E_a]$ is plotted versus time t for a given current, a linear relation is expected; the slope S of the line is

$$S = - \left(\frac{I^2 R'}{C_p} \right) \left(\frac{E_a}{E_{ss} - E_a} \right)$$

from which the heat capacity is easily found as

$$C_p = - \left(\frac{I^2 R'}{S} \right) \frac{E_a}{E_{ss} - E_a} \quad (E13)$$

This latter method has the advantage that exact knowledge of 0 time is not required, a problem which sometimes arose when currents were large and the circuit would "ring" somewhat, or when the skin effect in iron would create an initial hump in the voltage time trace.

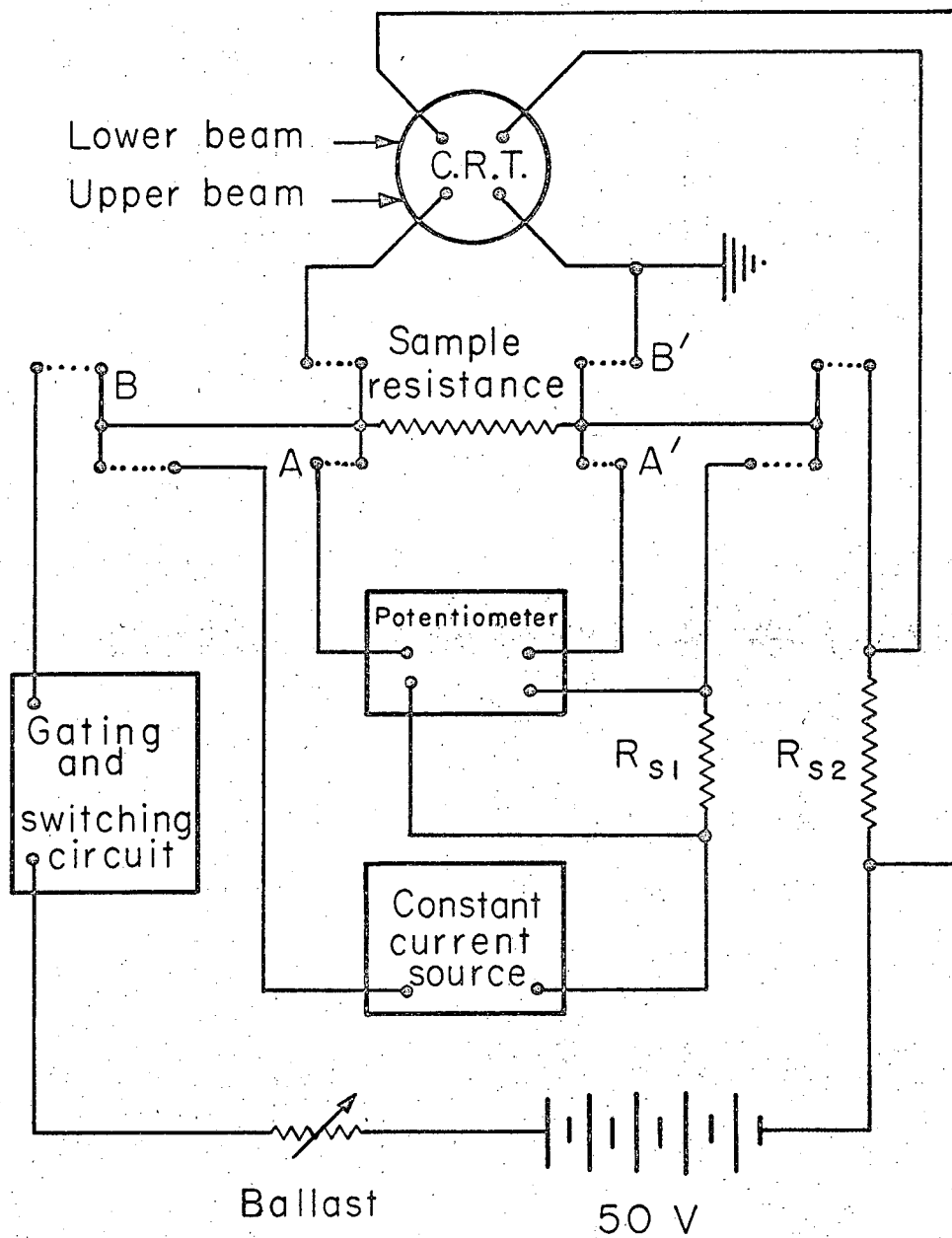
Both methods were used; the method characterized by Eq. (E5), referred to hereafter as Method I, was used more extensively because of convenience. The method characterized by Eq. (E13), referred to later as Method II, is somewhat heir to large errors because of the term $(E_{ss} - E_a)$, a small difference. Method II in particular delineated the

time scale necessary for these experiments. It was found that the sample could not be heated more than 1-2 milliseconds before heat transfer to the surroundings was sufficient to affect the results. This effect was shown by the fact that decreasing time scales (equivalent to a decreasing elapsed time from a point near $t = 0$) gave decreasing heat capacities until the 1 millisecond level was reached, at which point the heat capacity became relatively constant and independent of the time scale used. The heat loss at the longer time scans meant less energy into the sample, with the consequence an apparently larger heat capacity.

These results agreed with experience with method I: for nominal 2 ampere currents it was found necessary to use time scales of about 50 microseconds/cm (thus giving a total time scan of around 0.5 milliseconds) to obtain a linear trace. Beyond this time the trace began to exhibit the concave downward curvature characteristic of heat leak.

When the shorter time scales were used in both methods, agreement between the two is satisfactory to the degree allowed by the uncertainty in method II.

Examination of Eq. (E5) shows that the experimental data required to find C_p by method I are I , R , R' , and dE/dt . Figure 4 shows a block diagram of the apparatus used for these measurements. The apparatus essentially consists of two systems, one to measure a static EMF across the sample at low level direct currents, the other to measure a dynamic (time dependent) EMF using relatively large currents. Provisions for switching one system or the other to the sample are indicated by the dotted lines in the figure. To measure the dc electrical resistance of the sample the connections at A and A' are made; the potential across the sample was determined potentiometrically using one bank of a Leeds and Northrup White Double potentiometer with a sensitivity of ± 2 microvolt. The magnitude of the current passing



XBL672-941

Fig. 4 Block diagram of electronics.

through the sample was found from the potential across the standard 1 ohm resistor R_{s1} , utilizing the other bank of the potentiometer. The constant current source itself was usually a 12 volt auto storage battery in series with a high wattage variable resistor of nominal value 1200 ohms. By maintaining the battery in a reasonable state of charge a current of around 10 milliamperes constant to approximately .02% could be maintained for a period of 5 minutes. Dummy loads were provided for the supply during the time it was not connected to the sample. This steadied the discharge characteristics of the battery.

The resistance of the sample is easily obtained from the relation $R = E/I$ once E and I have been measured. Not indicated in the block diagram are provisions for reversing the direction of the current, a procedure necessary when working in the presence of a temperature gradient. In that event the average value of the resistance measured with positive current and that measured with negative I is taken to be the correct value; the thermal EMF cancels out. The dc resistance measurement is the most precise of the data taken in this work, with an estimate of $\pm 0.2\%$ given as the uncertainty.

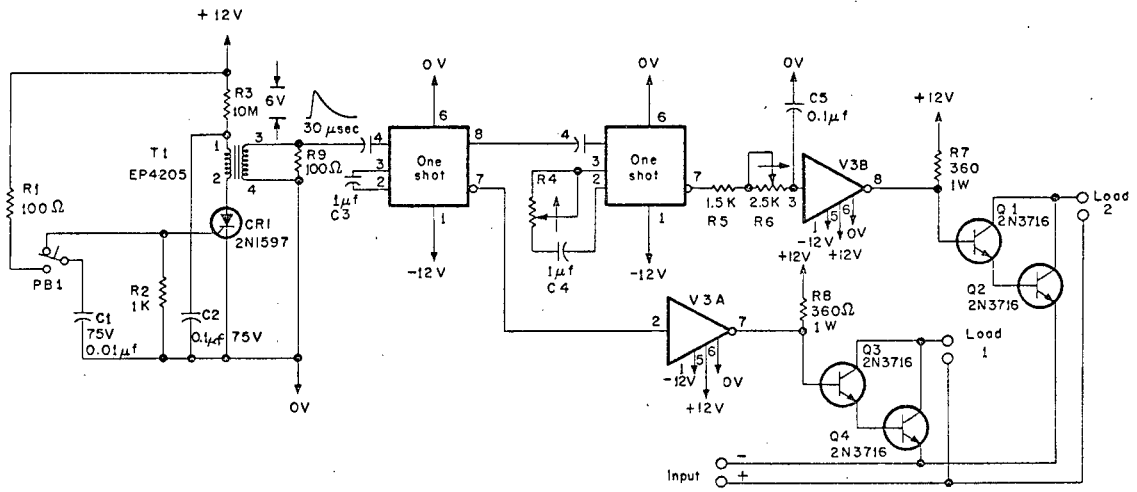
The circuit is connected at points B and B' for the dynamic measurement of the voltage across the sample. With the exception of the switching circuit, this configuration is analogous to the dc measuring circuit: The 50 volt bank of 12 volt auto storage batteries in series with the variable ballast resistor form a constant current source while the oscilloscope becomes the potential measuring device monitoring the EMF's across the sample and across the standard resistor R_{s2} . The latter measurement enables determination of the current I flowing through the sample for the duration of the pulse.

It was found experimentally that appreciable heat flow out from the sample had occurred in about 1-2 milliseconds under typical conditions. It was also known that large currents (2-10 amperes) could melt a portion of

the sample if applied for approximately 1 second. Thus the need for a pulsing technique was dictated, a technique in which a square current pulse with a fast rise time could be generated with a pulse width of something less than a few hundred milliseconds. A solid state switching device coupled to a battery-resistor current supply was the system developed to meet this need.

A battery-resistor supply for the constant current was found to be necessary in order to obtain fast rise time on the current pulse; rise times of 10 μ sec for current pulse of approximately 2.5 amps are achieved in the apparatus. The ballast resistance covered the range 5-400 ohms, giving a current range of .03-10 amperes. Sample resistances were of the order of .2 ohms; changes in the sample resistance were at most approximately .05 ohms. Thus a ballast resistance of 20 ohms resulted in a current of ~2.5 amps, and the increase of resistance due to the heating of the sample results in a current decrease of only ~6 milliamp, a few tenths of a percent. The current may be considered constant to this extent. Because of the higher currents required in this part of the experiment, repeated charging of the batteries was necessary for proper operation. Insufficient charge resulted in longer rise-time of the current pulse as well as a marked variation in the current during the pulse.

The solid state switching circuit generated the current pulse. Mechanical devices were found previously to be insufficient for the task because of speed and current carrying limitations. The device shown in Fig. 5 was developed for this purpose by the Special Problems Engineering group at Berkeley, under the direction of Paul Salz. There are actually two "switches" in the device, one for a dummy load and one for the sample. Each set of 2N3716 transistors is triggered by an EECO T-166 one shot multivibrator whose output pulse is amplified for switching purposes by the EECO T-170 relay driver. Pulse widths are determined by the charging rates of the external capacitors,



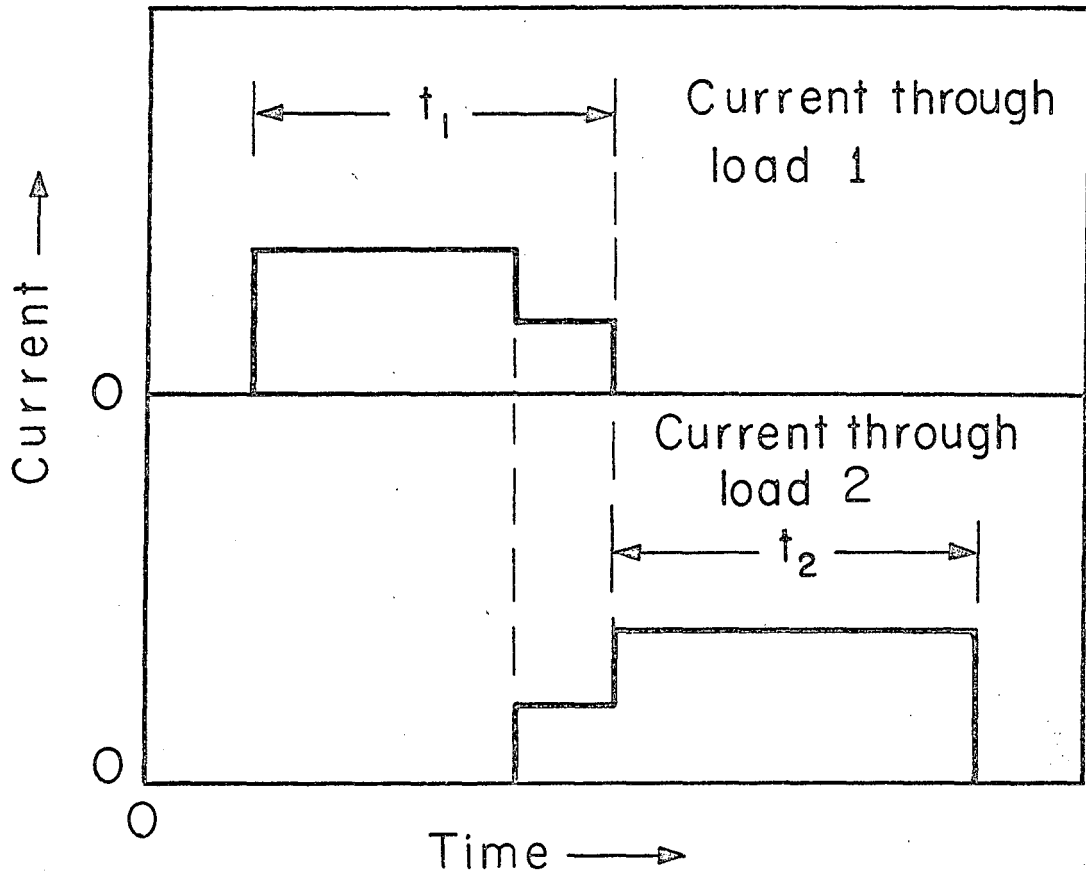
XBL 672 - 937

Fig. 5 Solid state switching circuit.

C3 and C4, on the one shots. The charging rate of capacity C4 of the sample (load 2 on the schematic) multivibrator is variable through resistor R4 to allow varying pulse widths. There is also a charging circuit on the output of the sample multivibrator to allow a delay in the firing of the sample transistors. The action of the device can be seen by examining Fig. 6, which shows the current output as a function of time for both the sample and the dummy loads. The current is first sent through the dummy load, a resistance of roughly the value of the sample resistance, in order to eliminate the transients and instabilities generated when the batteries first begin to deliver current. After a suitable time, about 10 milliseconds, the circuit through the sample is closed while current is still flowing in the dummy circuit. Then the dummy circuit is opened so all current flows through the sample. The rheostat R6 controls the charging rate of C5 and thus the overlap of the two pulses. In practice the overlap was minimized to diminish the additional heating of the sample during the overlap period.

The amplitude of the current pulse is determined from the voltage across the standard resistor R_{s2} , the resistance of which had been determined earlier to be 0.1 ohm. Thus a current of 1 amp resulted in an easily measured 100 millivolt signal at the oscilloscope. R_{s2} had a sufficiently high power rating and low thermal coefficient of resistance that during a pulse R_{s2} did not change appreciably in value.

Both the potential across the sample and the potential across R_{s2} were measured as a function of time on a Tektronix 555 dual beam oscilloscope. As indicated in the block diagram, the voltage across R_{s2} was measured differentially while the sample voltage was measured relative to a ground point which served as a reference for the entire system. The potential across R_{s2} may be measured with any amplifier having approximately .1 volt/cm sensitivity for differential determinations. In the present set up, a Tektronix type 1A7 amplifier is used because of its sensitivity and exceptional stability.



XBL672-942

Fig. 6 Schematic illustrating pulse generation in solid state switching circuit.

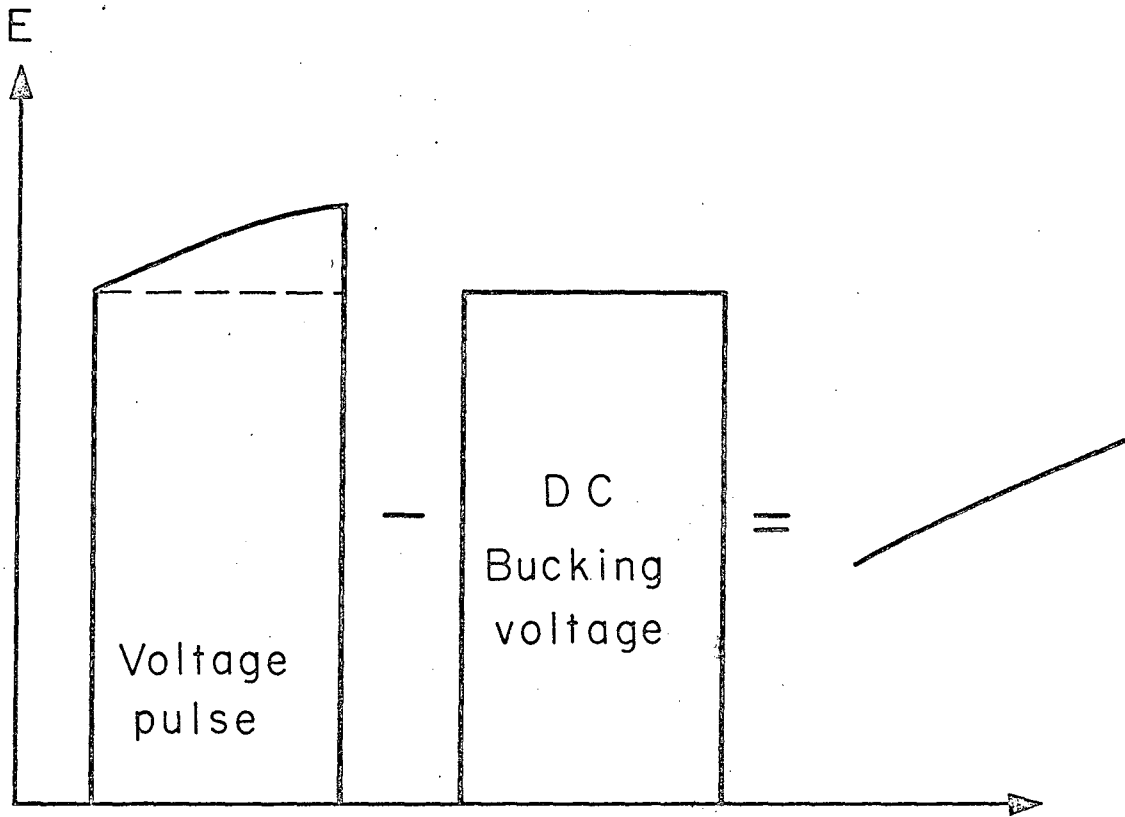
The sample potential was measured using the Tektronix Type W amplifier. This is a very stable, high gain differential comparator having a maximum sensitivity of 1 millivolt/cm. The internal comparison voltage enables one to examine the top of the voltage pulse at maximum sensitivity. For, as seen in Eq. (E5), one is interested only in the rate of change of the voltage, not the absolute magnitude. The situation is depicted graphically in Fig. 7: from the sample voltage pulse a dc voltage is subtracted, leaving only the top portion of the sample pulse to be examined at maximum sensitivity.

The sample voltage pulse was roughly Fourier analyzed. It was found that components above 100-300 kc were relatively unimportant while the lower frequencies played a larger role. It was most important to dc couple all amplifiers since the dc and low frequency components contributed a great deal to the wave shape.

Figure 8 shows a typical data record; the upper trace is the voltage across the sample, at 1 mv/div., the lower parallel traces give the current, at 1 amp/div. The time scale is 10 μ sec/division.

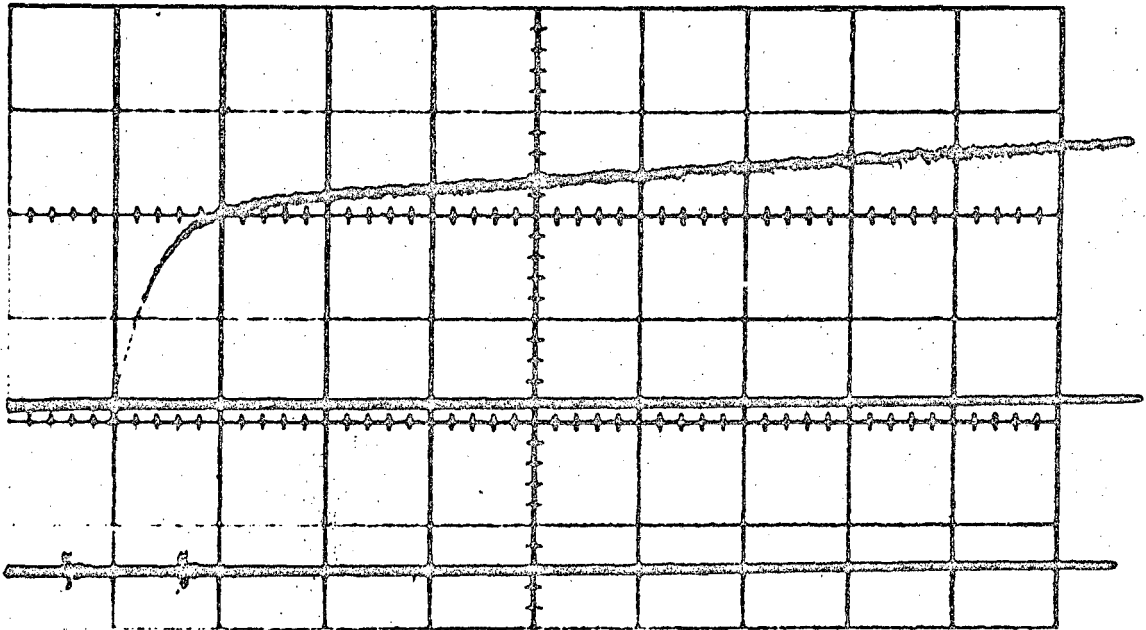
The traces were recorded by either of two methods. If records were made on Polaroid film, the various measurements of current and slope were made by hand, with the aid of a Gerber Variable Scale. To facilitate reduction of a large volume of data, some work was recorded on rolls of 35 mm Tri-X photographic film and measurements were made with the TRAMP II, a digitized protractor of the Heckman Visual Measuring group at Berkeley. Currents and slopes measured by hand have an estimated precision of $\pm 1-2\%$, while those done on the TRAMP are somewhat more precise. The oscilloscope time scales were calibrated to $\pm 1/2\%$ several times during the course of the research so the precision is assumed to represent the uncertainty in measuring distance on the photographs.

The high pressure generating apparatus is the opposed Bridgman anvil type used in these laboratories and described earlier.⁴⁸ A new grade of carbide, Kennametal K-68, was used for the anvil inserts with very good success. This



XBL672 - 943

Fig. 7 Schematic illustrating differential operation of Type ω amplifier.



XBL 673-1273

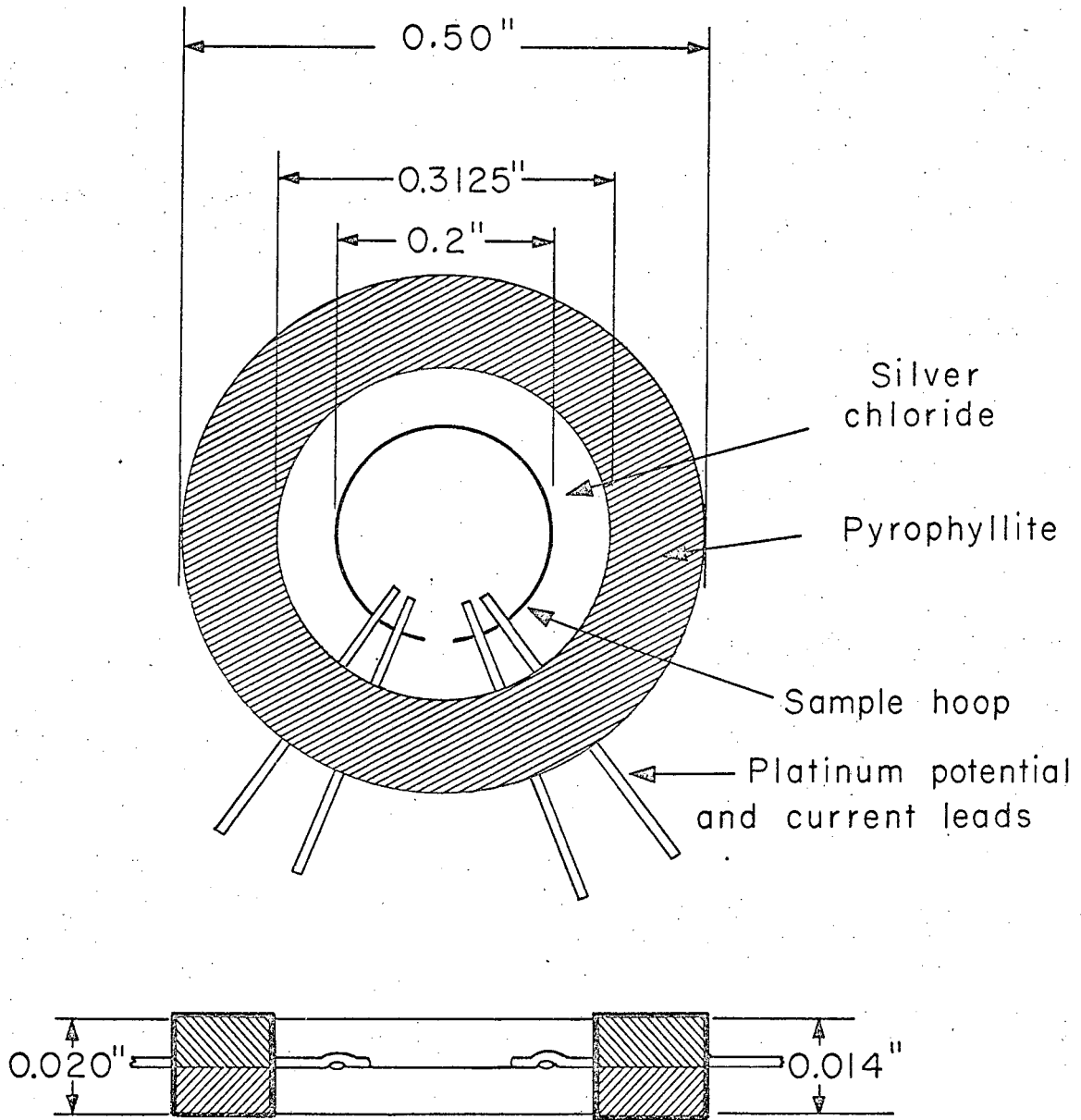
Fig. 8 A typical data trace.

material repeatedly was taken to 100 kb and over without fracture or noticeable deformation; no problems were encountered in the low temperature (77°K) runs, either.

The sample was contained in the four-lead, split-ring set up described by Stromberg and Jura,⁴⁹ modified by replacing the gold plug current inputs with another set of wire leads through the pyrophyllite wall. Figure 9 illustrates the sample "sandwich". Not shown in the figure is the .00025" mylar sheet fastened to the sides of the AgCl disks facing the sample. The mylar very effectively eliminated reaction between the metal sample and the corrosive silver chloride pressure transmitting medium without noticeably affecting the quasi-hydrostatic nature of the system.

The system pressure was monitored using a metal coil strain gauge and BLH strain indicator to measure the force applied by the hydraulic system. Calibration of the pressure scale was effected using the bismuth I-II and VI-VIII transitions, which have transition pressures of 25.4 kb and 88 kb, respectively.^{48,50} Since it is known that this type sample system is prone to radial pressure gradients,⁴⁸ all sample hoops were 0.2" in diameter and were placed concentric to the axis of the press. Calibration runs were made with 0.2" hoops also; all experiments and calibrations were made on compression runs only. The author presumes further that the fluidity of the silver chloride medium decreases with decreasing temperature. Consequently on those experiments where temperature was the variable parameter, the pressure was set at room temperature and while cooling or warming every effort was made to maintain constant loading. It is felt that the above techniques give a pressure scale which is accurate to at least $\pm 5\%$.

Temperature control has proven difficult for the Bridgman opposed anvil system, but progress is being made in eliminating temperature gradients which sometimes appear across samples which have been cooled to temperatures below 200°K in a simple dewar system. Early experiments⁵¹ to 77°K used massive copper blocks surrounding the sample and anvils inside a dewar to decrease



XBL672 - 944

Fig. 9 Schematic diagram of sample setup.

the temperature gradient from 20°K to $2-6^{\circ}\text{K}$. The technique is difficult for the four lead samples prepared in this research and was thus modified. A stainless steel can surrounded the loaded sample in the anvils. If the sample proved "good", i.e., if all electrical circuits were intact, approximately 75 lbs of fine No.12 lead shot was poured into the can, making a large heat sink. The sample itself was somewhat isolated by the use of Duxseal to prevent the lead shot from shorting out the leads. This system is essentially the equivalent of the copper blocks, although much easier to load (unloading is a little messy), and resulted in a temperature gradient of $\sim 2^{\circ}\text{K}$. While such a gradient seems to have little effect on the measured quantities (and indeed the effects may be further diminished by taking measurements with both positive and negative current flows), the rate of warming must be taken into account. Too high a rate inhibits taking data at meaningful increments. The above systems can warm as fast as $2-3^{\circ}\text{K}/\text{min}$; we have found that a reasonable rate is $0.1^{\circ}\text{K}/\text{min}$. Hence a move was made to liquid baths, in particular to the Kanolt solution bath described by Souers.⁵² This bath is usable only to about 150°K , but is much more convenient in terms of apparatus required than the methyl-butane system of Phillips,¹⁹ which could attain temperatures of $100-120^{\circ}\text{K}$. By the use of cooling coils carrying liquid nitrogen through the Kanolt bath, any desired warming rate could be achieved; actually it was found necessary to warm the bath with heaters as the temperature rose above 220°K , in order that the experiment did not take overly long. The bath was stirred with an air motor since electrical motors interfered with the triggering systems of the oscilloscope.

The temperature was measured using copper-constantan thermocouples which were spot welded or silver soldered to the anvil jackets, about 1-2" from the center. The thermocouples were all calibrated at 77°K in fresh liquid nitrogen, at 193°K in solid CO_2 , and at 273°K in crushed ice.

With the appropriate corrections made it is felt that temperatures are accurate to $\pm 0.1^\circ\text{K}$. The temperature gradient was usually $1/4$ degree or less.

The technique and procedure for taking data at a point along an isobar was the following. The temperatures of the top and bottom anvils were measured and recorded, and the voltage across the sample and current flowing through it were measured first with the current flowing one direction then in the other. The system was next switched to the oscilloscope and a series of about 15-25 pictures were taken at 5 or 6 different currents if the 35mm camera was used. Because of the time involved when the Polaroid camera was used only 8-15 pictures were taken at the various currents. Then the temperatures of the top and bottom anvils were measured again. Temperature rise for the whole sequence was $1/2^\circ\text{K}$ when the 35 mm camera was used, and somewhat more for the Polaroid. The average of the two sets of temperature data was used for the temperature of the heat capacity determination, while the average temperature of the first set of data was used in preparing the resistance temperature curve.

As mentioned earlier, if the E-t data were recorded on Polaroid film, the necessary measurements were made by hand whereas data taken on 35 mm film were measured on the TRAMP, which punches the appropriate coordinate data onto paper tape. Following conversion to magnetic tape on a DDP-24 computer, the 35 mm data was fed into the LRL IBM 7094 or CDC 6600 computer for reduction. A least squares linear fit was performed on the dE/dt and I^3 data for a given temperature. Points of poor fit (greater than 2.8 standard deviations away from the line) were discarded and a fit was attempted again, with the process repeated until suitable convergence was achieved. Polaroid data was generally fit graphically. The total data for a run was smoothed graphically, and often the temperature derivative of

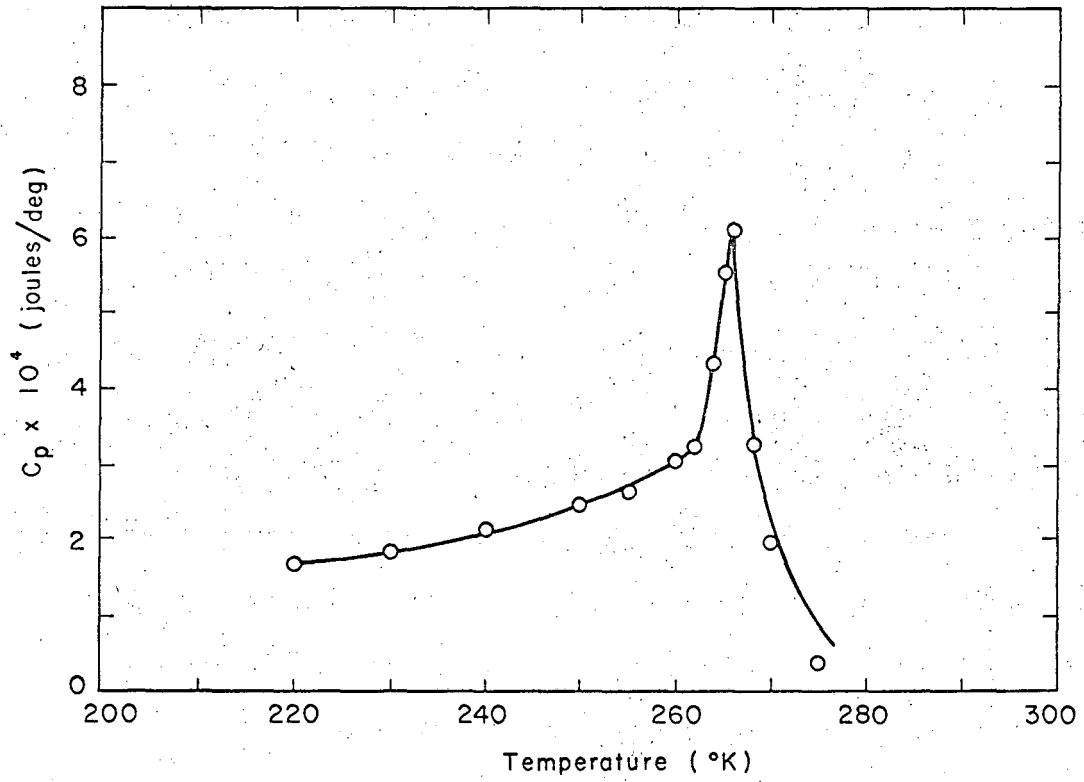
the resistance was calculated graphically by the chord area method. Final point by point calculations were carried out by hand on a desk calculator.

Results

The first investigation using the above apparatus was an examination of the heat capacity of gadolinium in the vicinity of the Curie temperature, T_c . At atmospheric pressure Gd undergoes the ferromagnetic-paramagnetic transition in the neighborhood of 292°K.⁵³⁻⁵⁵ The heat capacity anomaly occurs at 291.8°K with $\Delta C_p = 7$ cal/deg-mole.⁵⁵ This change of roughly 100% in C_p afforded a simple test of the apparatus.

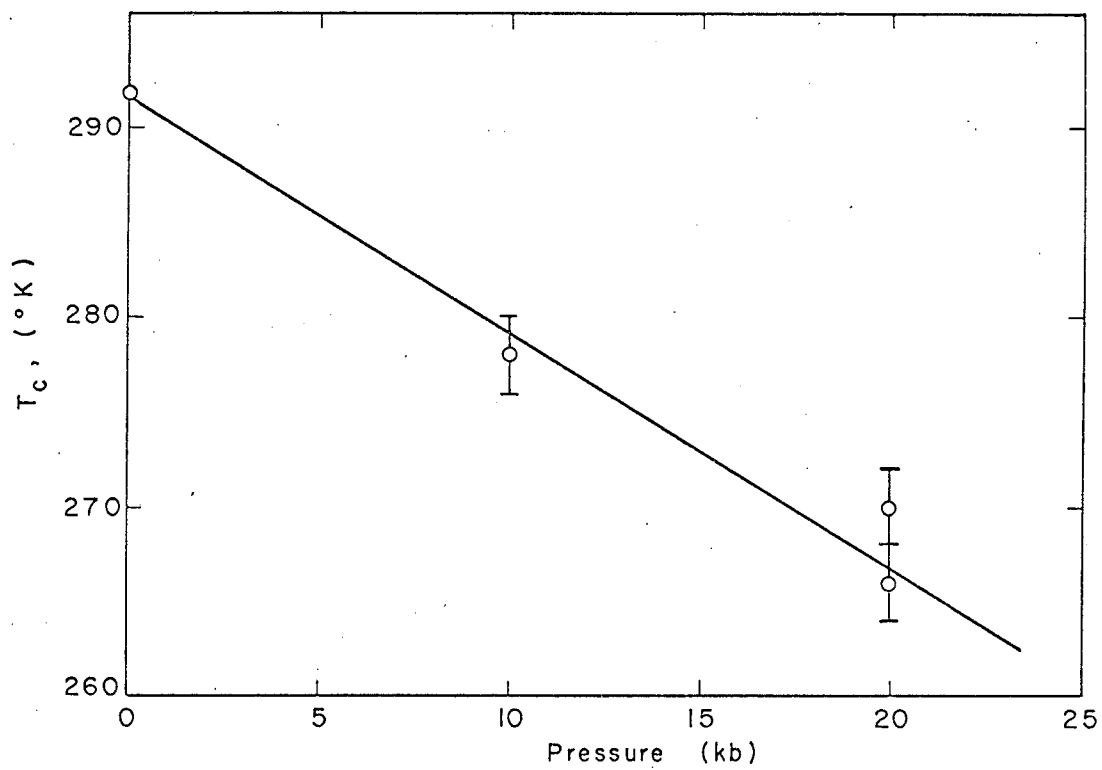
The gadolinium used was a portion of that studied by D. Phillips in this laboratory.¹⁹ The metal was supplied by Research Chemicals, Phoenix, Arizona; impurities of other rare earths and of transition metals were stated to be outside the limits of detection by spectrographic analysis.

Five separate runs were made in which two were in a sense less than successful, because the full width of the transition was not investigated. A relatively complete transition at 20 kb is shown in Fig. 10; a plot of transition temperature T_c versus pressure is shown in Fig. 11. The lower point at 20 kb is weighted more heavily because the two incomplete runs were at 20 kb and indicated that T_c at that pressure was somewhat lower than 270°K. As calculated from the graph $dT_c/dP = -1.3^\circ\text{K}/\text{kb}$, a value which is in good agreement with the literature values of -1.2 ,⁴¹ -1.53 ,⁴³ -1.6 ,⁴² -1.73 ,⁴⁴ and $-1.9^\circ\text{K}/\text{kb}$.¹⁹ Data was not extended to pressures above 20 kb since gadolinium is known to undergo a phase transformation to the samarium type structure at a pressure between 20-25 kb.^{42,44} Further analysis of the data, such as calculation of ΔH_{mag} and ΔS_{mag} , the magnetic enthalpy and entropy, respectively, was not possible because the limited temperature range did not allow separation of the lattice and electronic heat capacity.



XBL672-945

Fig. 10 Heat capacity of Gd through the Curie transition.



XBL672-946

Fig. 11 Curie temperature of Gd as a function of pressure.

For equation of state studies it is desirable to have a metal with both a large compressibility and a high characteristic temperature θ , so that the change in θ (or other parameter characterizing the stiffness of the lattice) would be as large as possible. Unfortunately, to some extent these two properties are mutually exclusive; one might intuitively associate a high compressibility with a low force constant, and hence from Eq. (T10), a larger compressibility means a lower θ . One desires furthermore a metal with a relatively large resistivity so that a reasonable size sample may be used; smaller electrical resistivities require making the physical dimensions of the sample small in order to increase the resistance. Finally, one would like a metal with a large temperature coefficient of resistance, so that temperature increases may be seen more easily.

The metal studied most extensively in this work was iron, which was chosen as having an optimized combination of the properties listed above; at room temperature and zero pressure, $\theta_D = 432^\circ\text{K}$,⁵⁶ $\chi = 5.826 \times 10^{-7} (\text{cm}^2/\text{kg})$,³⁸ $\rho = 9.8 \mu\Omega \text{ cm}$,⁵⁷ and $\frac{1}{R} \frac{dR}{dT} = 5 \times 10^{-3} \text{ K}^{-1}$.⁵⁸

Iron wire .003" in diameter and stated purity 99.9% from United Mineral and Chemical Company, New York, was used for the sample. Spectrochemical analysis confirmed the purity given above, although the technique used is not sensitive to carbon impurities. The wire was generally annealed at temperatures of 1100°K for several hours in either a good vacuum or a few mm of a 94% He-6% H₂ mixture. This was done mostly to make the wire easier to shape; little difference in resistance was found between the annealed and unannealed wire.

More than twenty separate runs were made, about half of which were isobaric runs at 20, 25, 30, 50, 75, and 100 kb. At least three room temperature isotherms to 100 kb and above were run, and these data were supplemented by points taken while increasing the pressure for some of the

higher isobars. The data of three isotherms at dry ice temperatures (195°K) showed good agreement with values calculated from the isobaric runs and the room temperature isotherms. (This result shows that it is possible to vary the pressure at lower temperatures, provided changes in P are made slowly, and provided that sufficient time is allowed for the system to come to equilibrium.)

It was found to be practically impossible to retain a given sample for more than one isobaric run; in only one case did the sample not blow out after warming to near room temperature. (It is probable that the cooling bath liquid penetrated the pyrophyllite ring, weakening it by decreasing the coefficient of friction. When the temperature rose to the point where the AgCl was sufficiently fluid, the blowout occurred.) It was therefore required to relate the various runs to one another. The effect of sample size was eliminated by using reduced resistances and slopes (henceforth the symbol S will be used to denote the slope of a dE/dt vs I^3 plot). The isothermal R and S data enabled one to tie the isobaric runs together.

The experimental data are:

$$\frac{R(P, 295)}{R(20, 295)} \quad \text{vs } P \text{ at } 295^\circ \text{K}$$

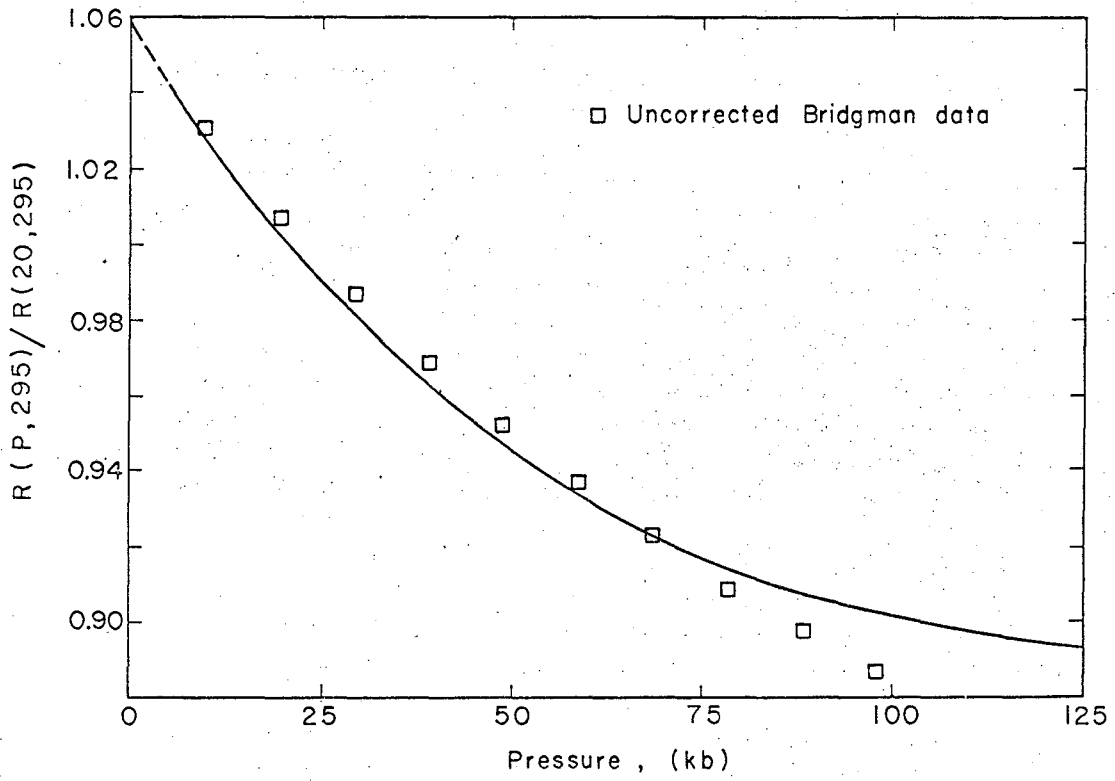
$$\frac{R(P, T)}{R(P, 200)} \quad \text{vs } T \text{ at } P$$

$$\frac{1}{R(P, 200)} \cdot \frac{dR(P, T)}{dt} \quad \text{vs } T \text{ at } P$$

$$\frac{S(P, 295)}{S(20, 295)} \quad \text{vs } P \text{ at } 295^\circ \text{K}$$

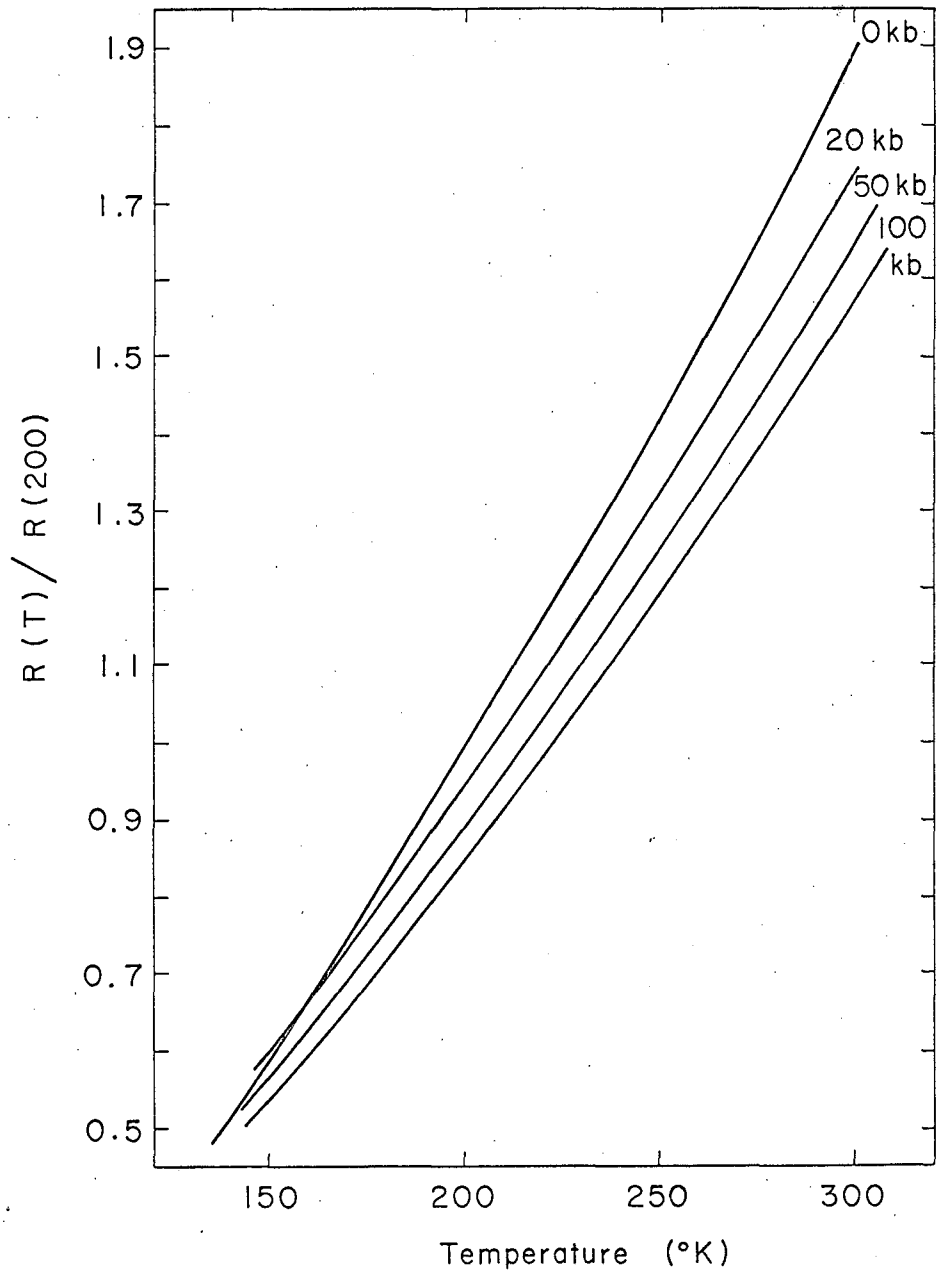
$$\frac{S(P, T)}{S(P, 200)} \quad \text{vs } T \text{ at } P$$

200°K was a common point for all isobaric runs. The data is shown in Figs. 12-19. Figure 12 illustrates the room temperature resistance isotherm, $R(P, 295)/R(20, 295)$ vs pressure; the solid line is a least squares polynomial fit of the data of this work, and the squares are from Bridgman's opposed anvil data.⁵⁹ The agreement is satisfactory in view of the fact that Bridgman, unaware of the pressure gradient in the ring system, used



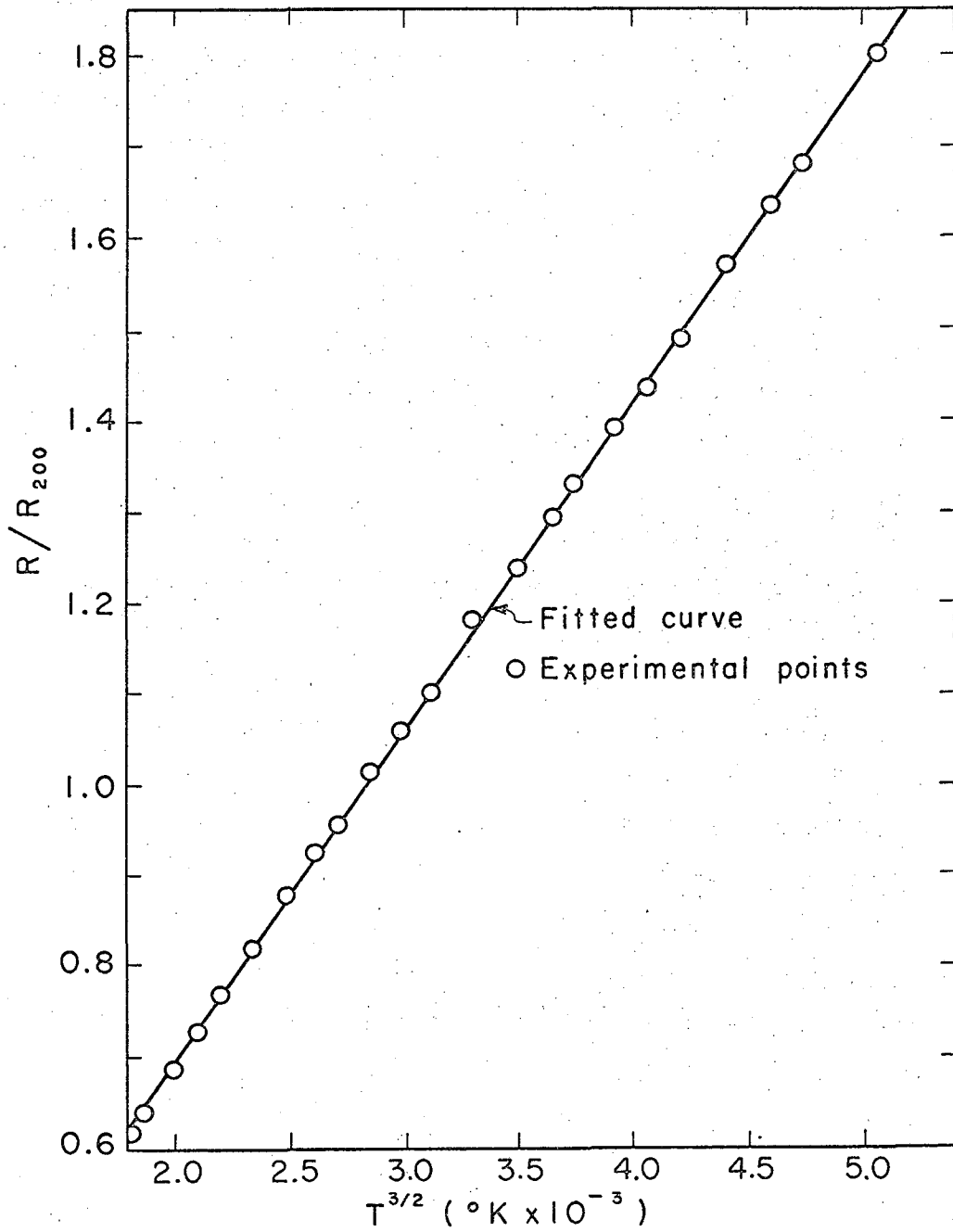
XBL672-947

Fig. 12 Room temperature resistance isotherm of iron.



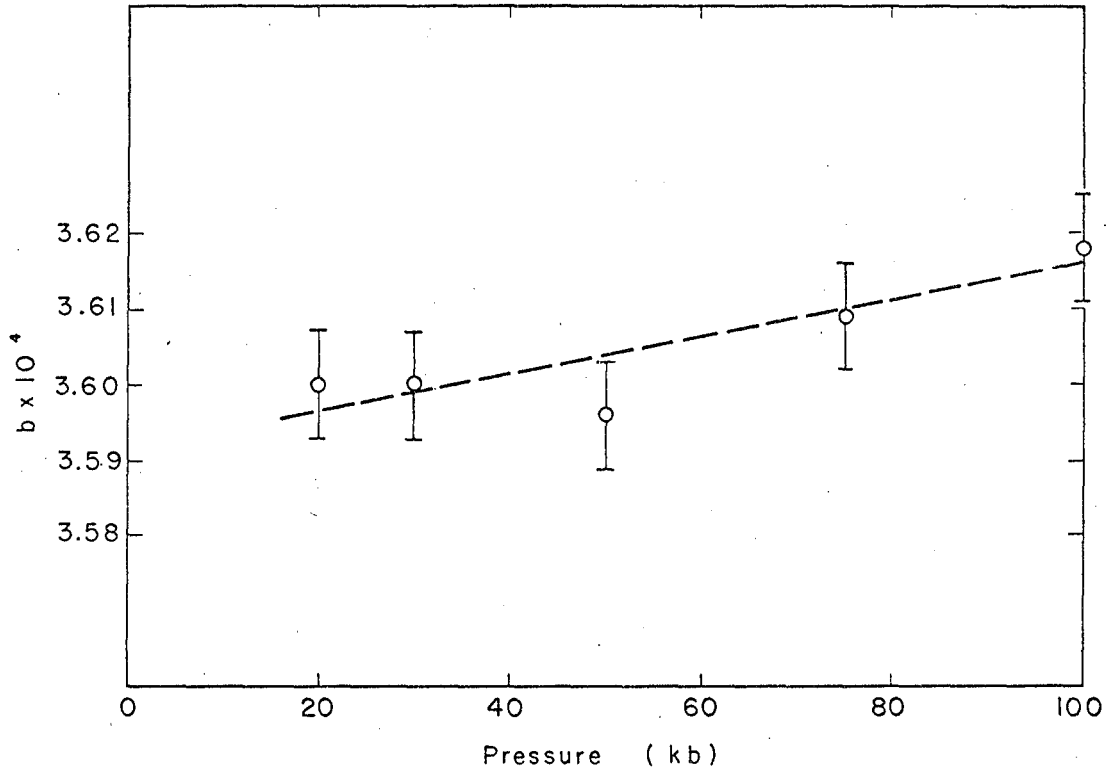
XBL673-2260

Fig. 13 Resistance isobars of iron.



XBL 672-949

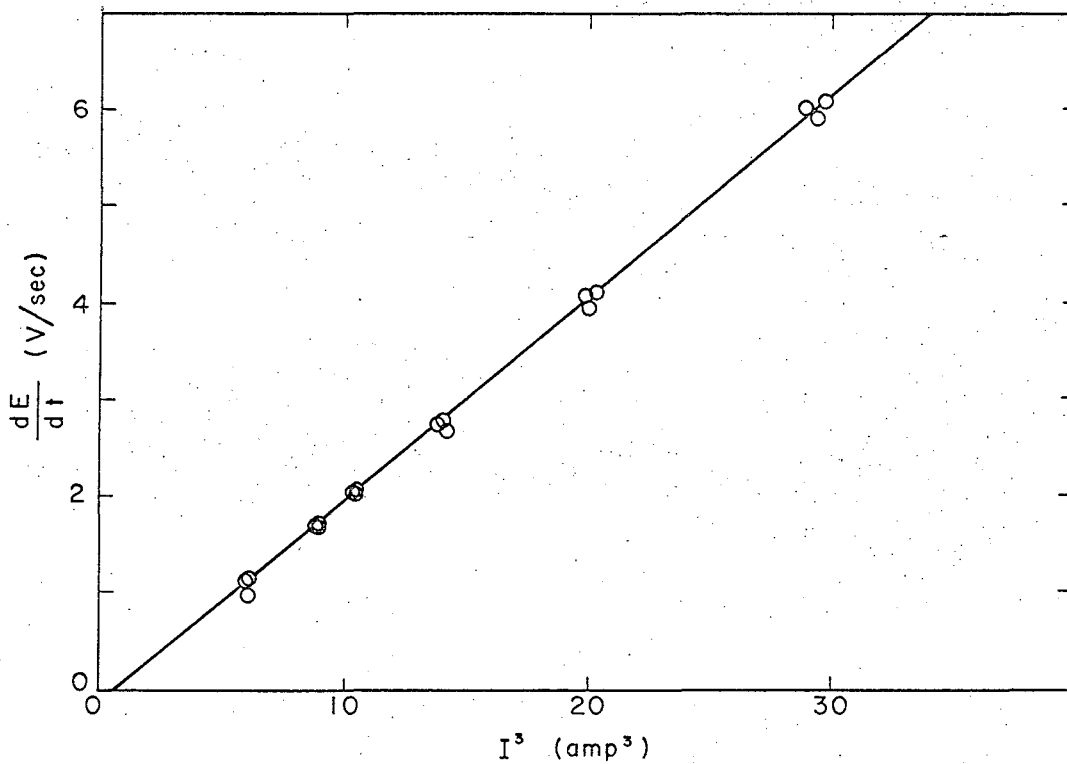
Fig. 14 20 kb resistance isobar of iron, plotted versus $T^{3/2}$.



XBL672-950

Fig. 15 Temperature derivative of resistance of iron;

$$1/R_{200} - dR/dT = 3/2 bT^{1/2}.$$



XBL672-948

Fig. 16 Typical dE/dt versus I^3 plot for iron.

a sample strip straight across the ring. This technique results in pressures lower than the applied pressure (defined as the applied force divided by the area of contact) by a variable factor of around 0.8.⁴⁸ Distortion of the anvil faces at high pressures may also give discrepancies.

A composite graph of $R(P,T)/R(P,200)$ is shown in Fig. 13, and it can be seen that the temperature dependence of the reduced resistance is very nearly the same for all pressures of 20 kb and greater. The 0 kb data was taken from the work of White and Woods;⁵⁷ the intersection of the 20 kb isobar of this work with their atmospheric values at 150°K most likely is due to a difference in purity of the iron used in the two studies. It was found experimentally that the reduced resistance of iron at $P \geq 20$ kb was proportional to $T^{3/2}$; the implications of this find are discussed in Appendix I. The data for 20 kb are presented in this fashion in Fig. 13, which includes the experimental points as well as the computed line. The slight differences in the R curves are best seen in the derivative. If one assumes that $R/R_{200} = a + bT^{3/2}$, then the derivative is given by $(1/R_{200})dR/dT = 3/2 bT^{1/2}$. A graph of b versus pressure is shown in Fig. 14. The dashed line is a least squares fit by the equation

$$b = 3.592 \times 10^{-4} + 2.35 \times 10^{-8} P,$$

for P in kb. The fit is valid only for $P \geq 20$ kb, since at lower pressures the exponent of T in the resistance function increases. The increase in b with pressure represents a slight stiffening of the lattice.

The slope S is found from the dE/dt vs I^3 graphical plots or numerical fits. A typical dE/dt vs I^3 plot for iron is shown in Fig. 15; the linear fit is quite good and error analysis⁶⁰ indicates a probable error of 1-2% in the slope; the uncertainty in measuring data off of the photographs leads to an uncertainty of 3% in I^3 and of 2-3% in dE/dt . Note that the line does not intercept the origin; in this graph, as in the majority of the plots, the intercept is negative. The magnitude of the intercept is also usually outside the limits of experimental error. A series of experiments on iron, somewhat

uncertain because of the inability to determine small values of dE/dt with good precision, showed no curvature to meet the origin. The behavior of the intercept with varying pressure or temperature is not particularly regular, and no explanation save some systematic error can be given at this time. The intercept is treated in this work as a constant heat leak; hence the slope S of the linear dE/dt vs I^3 graph is used to calculate C_p .

Figure 17 is the $S(P)/S(20)$ 295°K isotherm; the solid line is a least squares polynomial fit of all data, while the various points indicate the degree of scatter. All data lie within 2.5 standard deviations from the fitted curve, with $\sigma = 2.8 \times 10^{-2}$. Finally, in Fig. 18, the slope data $S(P,T)/S(20,295)$ for iron are presented. Like the resistance data these last data show little difference from pressure to pressure when displayed in reduced form.

All heat capacities were computed relative to the heat capacity at 20 kb and 295°K. The method of calculation is the following:

From theory (Eq. (E5)) the heat capacity at pressure P and temperature T is given as

$$C_p(P,T) = \frac{R(P,T) \cdot R'(P,T)}{S(P,T)}$$

and at $P = 20$ kb, $T = 295^\circ$ K,

$$C_p(20,295) = \frac{R(20,295) \cdot R'(20,295)}{S(20,295)}$$

The ratio of these two heat capacities is therefore given by

$$\frac{C_p(P,T)}{C_p(20,295)} = \frac{R(P,T)}{R(20,295)} \cdot \frac{R'(P,T)}{R'(20,295)} \cdot \frac{S(20,295)}{S(P,T)} \quad (E2)$$

Each of the three terms on the right may be expressed in terms of the measured quantities:

$$\begin{aligned} \frac{R(P,T)}{R(20,295)} &= \frac{R(P,T)}{R(P,200)} \cdot \frac{R(P,200)}{R(P,295)} \cdot \frac{R(P,295)}{R(20,295)} \quad (E3) \\ &= \frac{R(P,T)}{R(P,200)} \cdot \frac{R(P,295)}{R(20,295)} \cdot \frac{R(P,295)}{R(P,200)} \end{aligned}$$

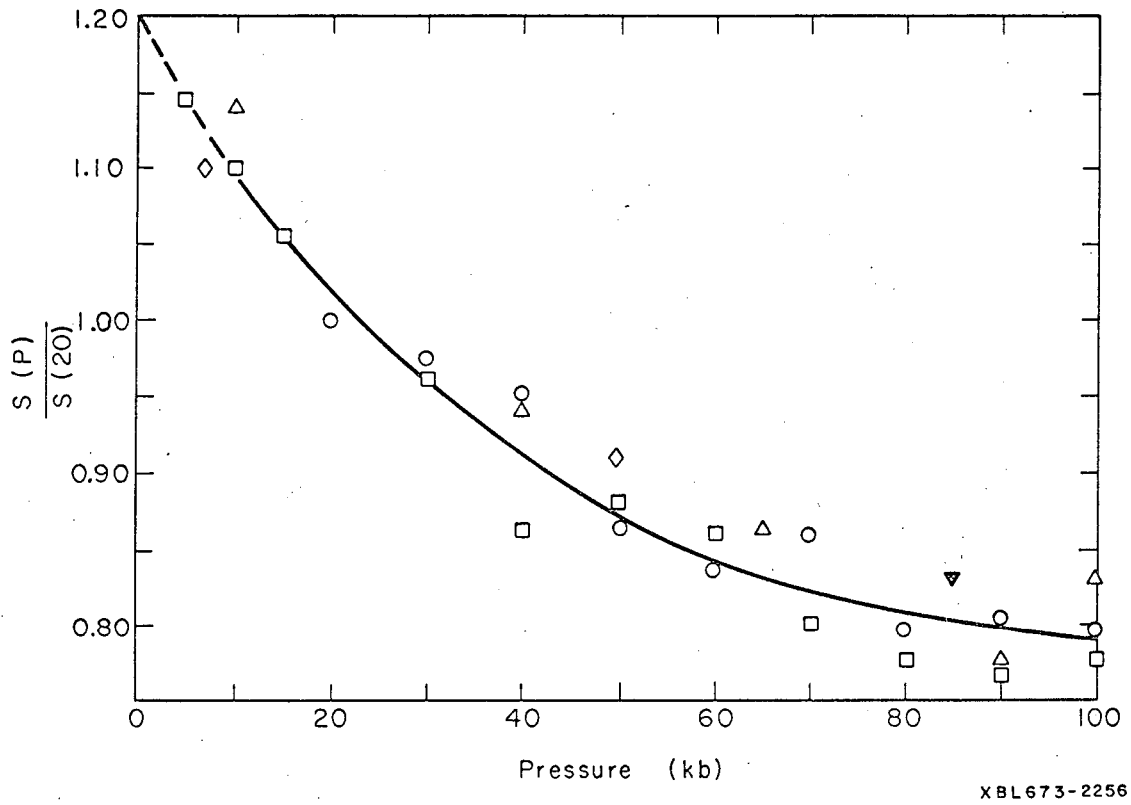
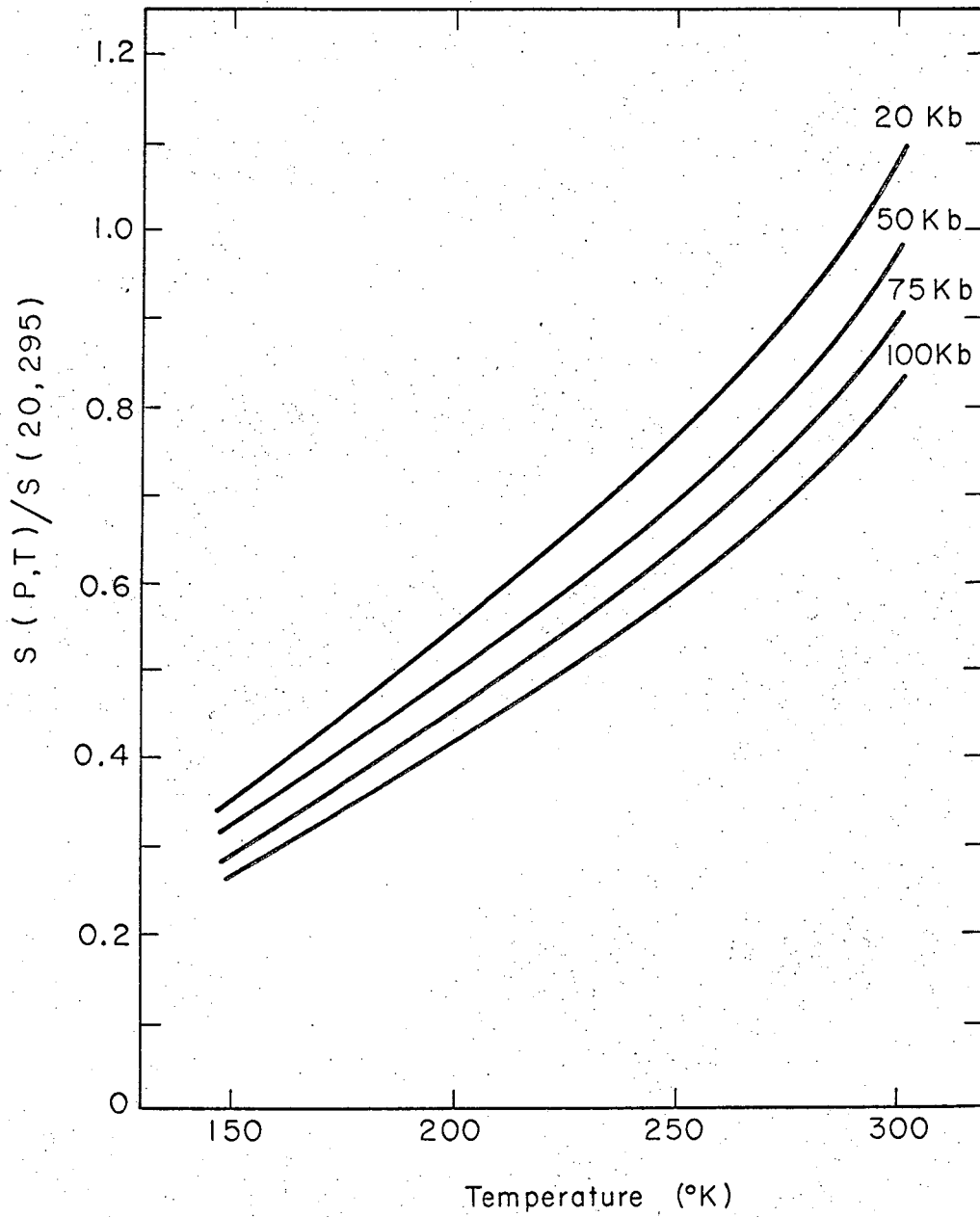


Fig. 17 295°K isotherm of slope data for iron.



XBL 673-2257

Fig. 18 Slope isobars for iron.

$$\begin{aligned}
 \frac{R'(P,T)}{R'(20,295)} &= \frac{R(P,200)}{R(20,200)} \cdot \frac{\frac{R'(P,T)}{R(P,200)}}{\frac{R'(20,295)}{R(20,200)}} \\
 &= \frac{R(P,200)}{R(P,295)} \cdot \frac{R(P,295)}{R(20,295)} \cdot \frac{R(20,295)}{R(20,200)} \cdot \frac{\frac{R'(P,T)}{R(P,200)}}{\frac{R'(20,295)}{R(20,200)}} \\
 &= \frac{\frac{R'(P,T)}{R(P,200)} \cdot \frac{R(P,295)}{R(20,295)}}{\frac{R(P,295)}{R(P,200)}} \cdot D \quad (E4)
 \end{aligned}$$

where

$$D = \frac{\frac{R(20,295)}{R(20,200)}}{\frac{R'(20,295)}{R(20,200)}}$$

and is a constant for any given metal.

$$\begin{aligned}
 \frac{S(20,295)}{S(P,T)} &= \frac{S(20,295)}{S(P,295)} \cdot \frac{S(P,295)}{S(P,200)} \cdot \frac{S(P,200)}{S(P,T)} \\
 &= \frac{\frac{S(P,295)}{S(P,200)}}{\frac{S(P,295)}{S(20,295)} \cdot \frac{S(P,T)}{S(P,200)}} \quad (E5)
 \end{aligned}$$

On combining Eqs. (E3), (E4), and (E5) one finds the ratio of heat capacities in terms of reduced variables as

$$\frac{C_p(P,T)}{C_p(20,295)} = \frac{\frac{R(P,T)}{R(P,200)} \cdot \frac{R'(P,T)}{R(P,200)}}{\frac{S(P,T)}{S(P,200)}} \cdot M(P) \cdot D \quad (E6)$$

$$M(P) = \left(\frac{\frac{R(P,295)}{R(20,295)}}{\frac{R(P,295)}{R(P,200)}} \right)^2 \cdot \left(\frac{\frac{S(P,295)}{S(P,200)}}{\frac{S(P,295)}{S(20,295)}} \right)$$

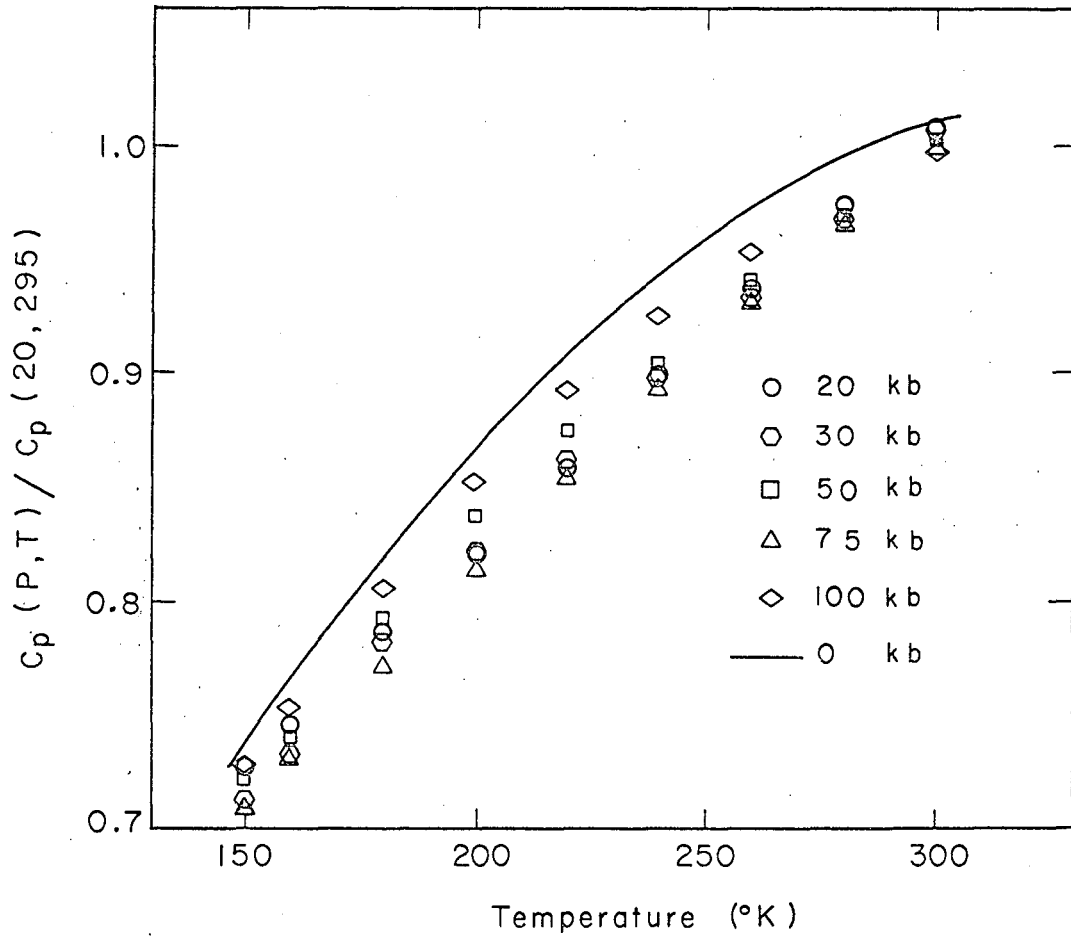
and is seen to be a function of pressure only.

The isobaric runs were calculated according to Eq. (E6). The isobars were tied together at 295°K using the additional results of 6 isotherms which indicated a 1% drop in C_p from 25 to 100 kb, and which, if linearly extrapolated to zero pressure, indicate that $C_p(0,295)$ is approximately 1% greater than $C_p(25,295)$. The spread of data is such that one could say the heat capacity remains constant from 0-100 kb at 295°K; however, by using the thermal expansion data of Nix and McNair,⁶¹ and by assuming that ΔC_p is given approximately by

$$\Delta C_p \sim \left(\frac{\partial C_p}{\partial P} \right)_T \cdot \Delta P = -T \left(\frac{\partial^2 V}{\partial T^2} \right)_{p=0} \cdot \Delta P \quad (E7)$$

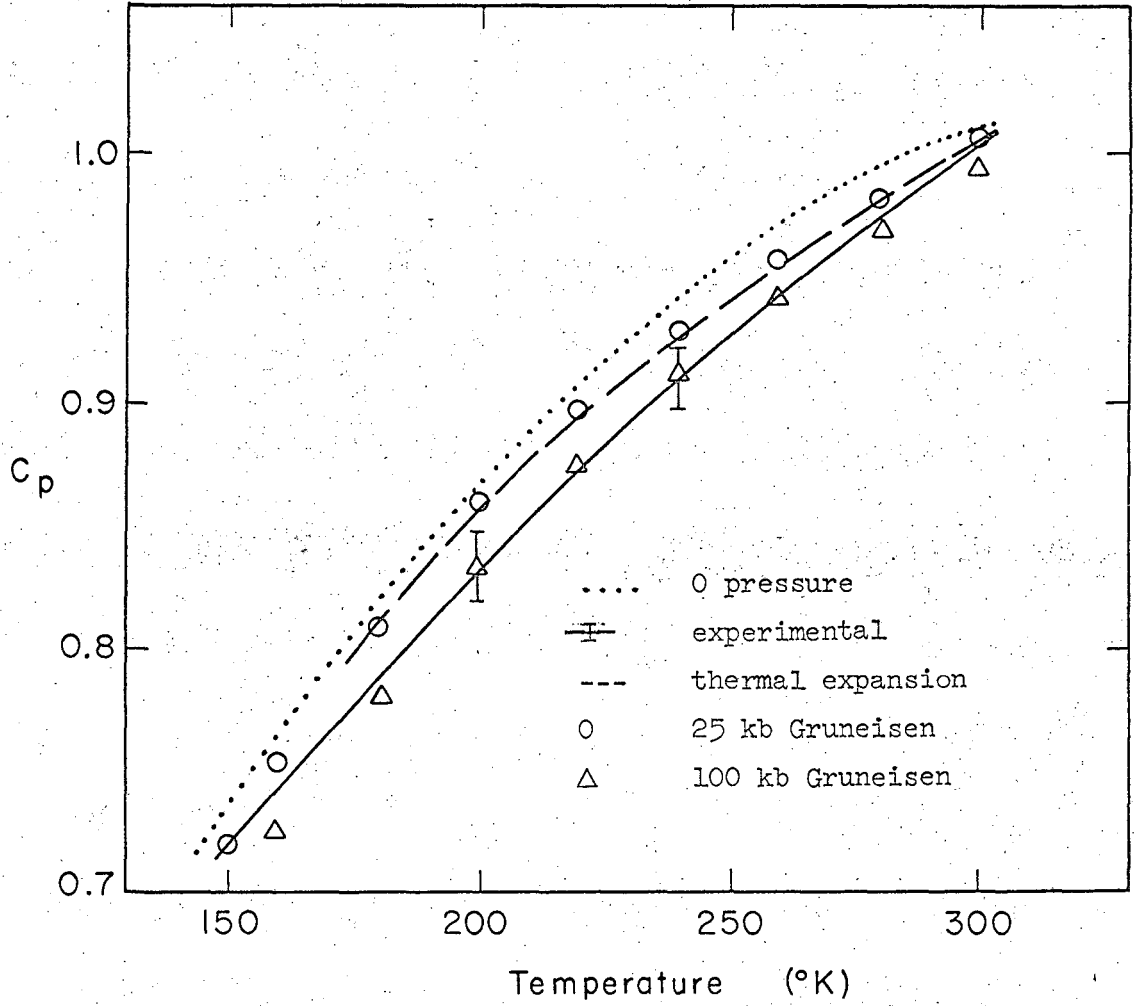
one finds the heat capacity at 0 pressure is about .8% greater than at 25 kb.

The data connected in the above fashion is shown in Fig. 19, along with the zero pressure data of Kelley.^{62,63} The scatter among the experimental points is approximately $\pm 1\%$ at the worst, and the data indicate no regular progression with pressure. Hence the data is treated as independent of pressure, and averaged to give the graph of Fig. 20, again including the atmospheric pressure data. Also shown in Fig. 20 are the C_p curve at 25 kb calculated from the thermal expansion data of Nix and McNair using the relation (E7), a C_p curve at 25 kb calculated in the Grüneisen approximation with $\gamma = 1.70$ and independent of volume; the assumption that the electronic and magnetic heat capacities were independent of pressure was made in this calculation as in the identical calculation of the C_p curve at 100 kb. The experimental data average lies in the region bounded by these approximations.



XBL673-2258

Fig. 19 Experimental heat capacity isobars of iron.

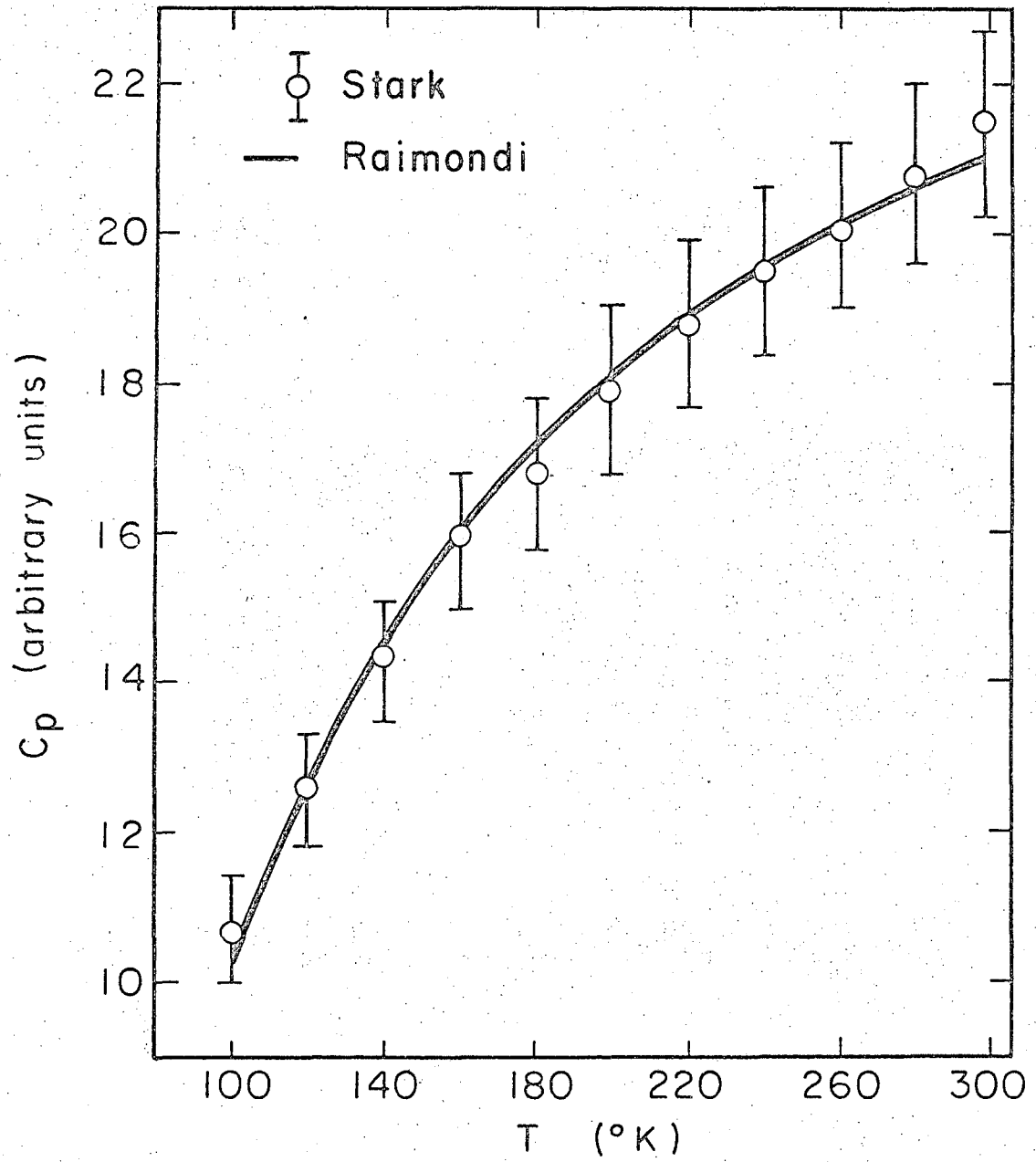


XBL673-2259

Fig. 20 Experimental heat capacities of iron compared with various approximations.

Within the 5-6% uncertainty of the experimental data then, the heat capacity C_p of iron definitely does not change in the pressure range 20-100 kb. Moreover, although no experimental comparison was possible, it is probable that the difference between the high pressure heat capacities and the zero pressure value is small. It appears that a Grüneisen type approximation, with a γ which is independent of volume, is sufficient to describe the thermodynamic behavior of the iron lattice as a function of pressure; the assumption of constant magnetic and electronic is apparently reasonable, and at any rate introduces only a small error since these two heat capacities are only small components of the total in the temperature region investigated.

Because of the apparent small variation in the heat capacity of iron at high pressures, an attempt was made to measure the heat capacity of aluminum, which is known to exhibit a 6% decrease in C_p at room temperature,¹⁰ and the greater increases attendant at lower temperatures. Some degree of success was had in the isobaric runs, as shown in Fig. 21, which compares measured values at 50 kb with the result of calculations using Raimondi's equation of state. The agreement is good, but somewhat misleading since a $\pm 20^\circ$ variation in θ will still fit the curve within experimental error. The room temperature isothermal runs disagreed badly with existing theories in that an increase in C_p was found, the heat capacity at 100 kb being about 1.7 times the zero pressure value. It is not known at present exactly why the method should give these apparently unreasonable results, but the following observations and conclusions can be made. The first is that on the basis of $\log (dE/dt)$ vs $\log (I)$ linear plots, dE/dt was not proportional to I^3 as required by the theory developed earlier and shown by the iron and gadolinium work; rather it was found that $dE/dt \propto I^{3.7}$, approximately. This behavior, the exponent of I being greater than 3 is what one would



MUB 12108

Fig. 21 50 kb. heat capacity isobar of Al.

expect to find if there were a large heat leak. Because of the low resistivity of the aluminum the samples had to be made very small (.0005" thick) to have a resistance of usable magnitude. This resulted in a sample smaller, mole wise, than the iron samples by about an order of magnitude. A smaller sample heats more rapidly for a given power input; hence the point at which heat leakage becomes excessive is reached earlier. Higher currents were required in the aluminum work in order to develop significant potentials across the sample and it is possible that during the period of overlap of current flow through the dummy and sample resistances sufficient heat was generated in the sample to complicate the resulting measurements. Also, it has been noted experimentally that the higher currents have slower rise time, making it somewhat more difficult to ascertain the limiting slope on the dE/dt vs I^3 plots.

Conclusions

The experiments reported here show that it is possible to measure the heat capacities of metals under pressure with some measure of certainty. The results of the gadolinium experiment and the iron and aluminum isobars indicate that the method works reasonably well if the heat capacity changes are large; the experimental uncertainty of around $\pm 5\%$ sets a lower limit to the resolution of the present apparatus.

Some difficulty was brought to light in the isothermal experiments where sometimes in the case of iron a slight increase in C_p was noted on pressure increase, albeit within experimental error. The aluminum isotherms show a very definite increase in C_p as the pressure is increased, in contradiction with present theories and experimental work. Part of the difficulty is the low electrical resistivity of aluminum, but it is felt that there might also be some pressure dependent heat leak function which could

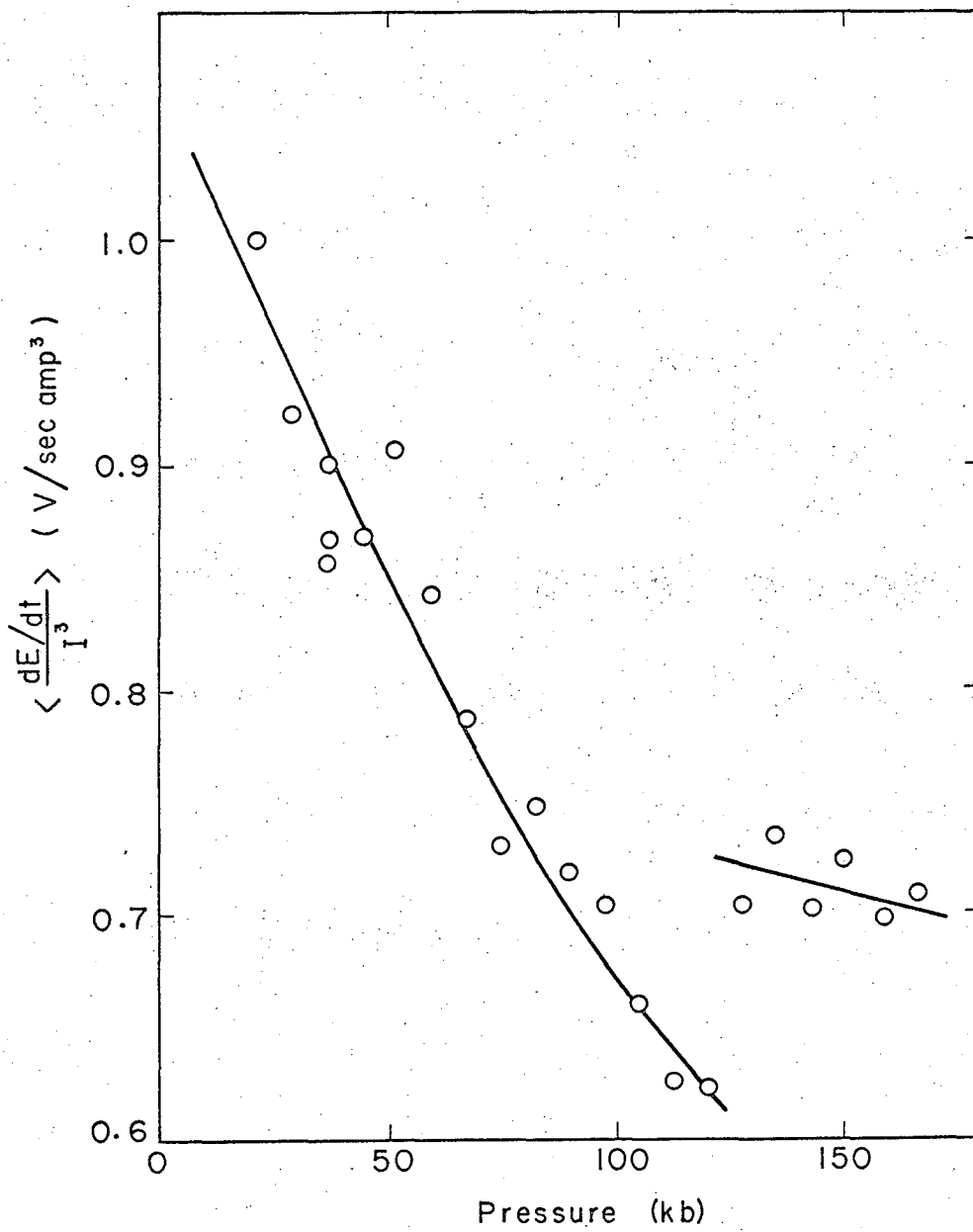
give rise to this effect. The nature of this function is as yet undetermined.

Another puzzling inconsistency which could be related to the above problem is the fact that the dE/dt vs I^3 relation, while actually linear as required by simple theory, experimentally does not give a zero intercept; the common result is that for $I^3 = 0$, $dE/dt < 0$. This result may be interpreted as a heat loss, and in this thesis it was assumed to be a constant. It possibly may be a more complicated function. Additional evidence that this negative intercept might represent a heat loss comes from some preliminary experiments done outside the pressure cell, where one would expect the heat loss term to be very much smaller. In these cases the dE/dt line was found to pass through the origin.

Future research thus has several directions. One is a clarification of the heat loss problem, both as a function of pressure, and at a given pressure and temperature. Many of the problems outlined above could be investigated more thoroughly when sensitive differential preamplifiers can be developed to allow use of larger samples and lower heating currents. Hopefully present limitations of the technique to metals having resistivities greater than about $5\mu\text{ohm cm}$ could be relaxed with such preamps.

Since the variation of the heat capacity with temperature is much greater than its apparent isothermal variation, the heat capacity work reported here would benefit greatly by an extension of the temperature range used. To this end a more elaborate temperature control system is necessary, and the author envisions a combination of the massive heat sink and liquid bath techniques to allow a temperature range from 65°K to over room temperature. Included in this control system should be some automatic load maintaining mechanism to prevent pressure drift when heating or cooling.

As it appears that isothermal variation of the heat capacity is relatively small, a more fruitful direction of research using heat capacities measured at high pressures might center on studies of phase changes under pressure. The gadolinium work presented here is one such study; further studies on gadolinium at higher pressures could give insight into the nature of the samarium type structure which appears above 25 kb. There are numerous other possibilities; Fig. 22 shows a $dE/dt/T^3$ isotherm for iron. The break at approximately 120 kb reflects the phase transition to the hcp structure at that pressure. Measurement of the resistance and temperature derivative of the resistance of the high pressure phase would allow the interesting calculation of the change in heat capacity across the phase boundary.



XBL672-951

Fig. 22 295°K slope isotherm for iron.

PART II. THERMAL SHOCKING

Many substances exhibit polymorphism under pressure, with the different phases most often having different physical characteristics such as volume, electrical resistance, magnetic permeability, etc., which enable identification of the particular phase. The problems of finding new phases and delineating their existence in P-T diagrams is a continuing one in high pressure research.

Quite often it is found that phase transitions are sluggish, and in some cases, for instance the Fe transition, super pressures of 20-60 kbars are required to complete a transition. Furthermore, even for a relatively "sharp" transition it can be argued that the observed isothermal transition pressure is greater than the thermodynamic pressure. The problem was recognized by Bridgman,⁴ who termed the region between the transition pressure on compression and the transition pressure on decompression as the region of indifference. Bridgman's region was widened additionally from friction effects in the pressure generating apparatus; he chose as the thermodynamic transition pressure the average of the compression and decompression values.

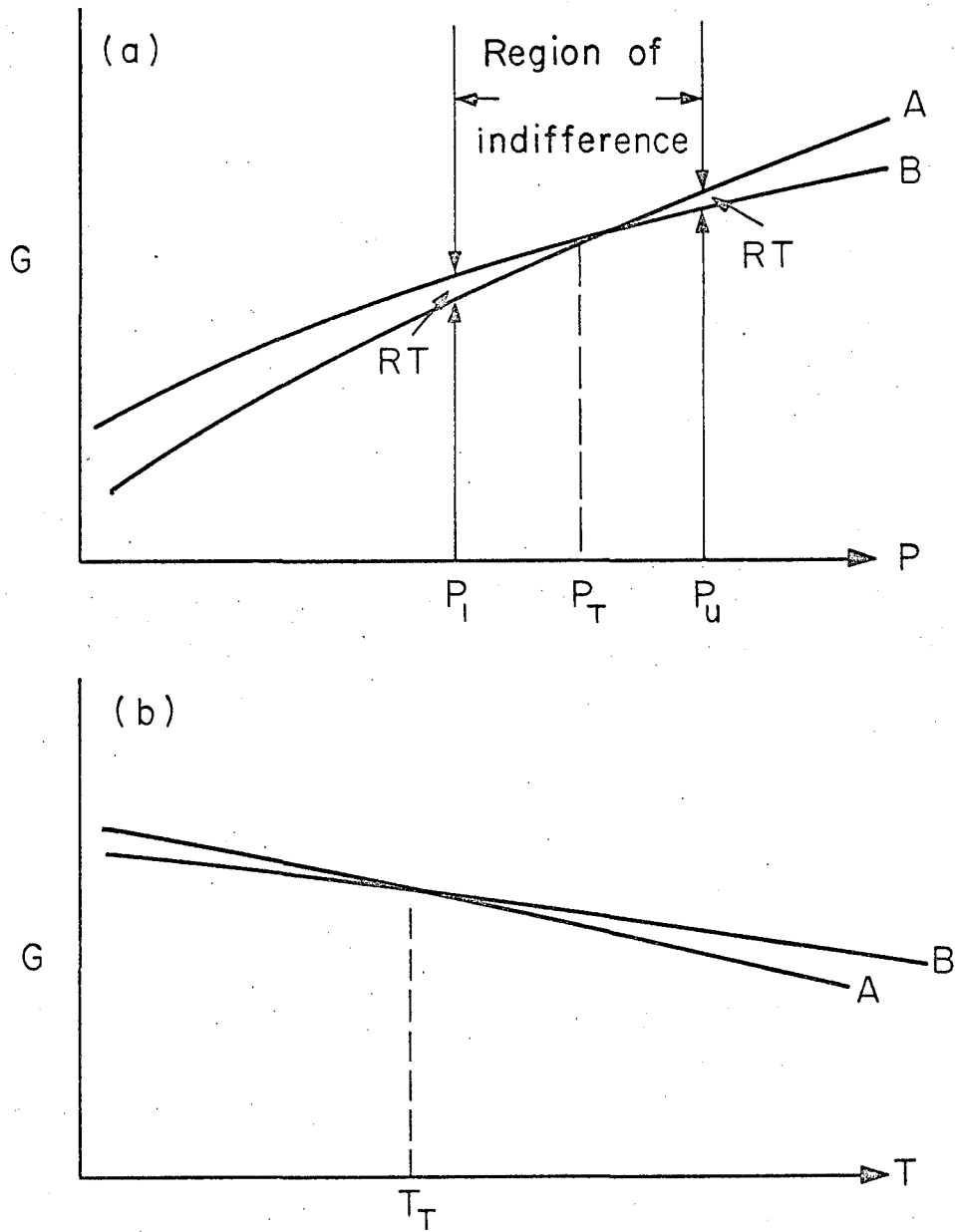
More recently, Kennedy and La Mori⁵⁰ obtained transition pressures which are probably quite close to the thermodynamic value; a shearing technique greatly decreased the difference between the compression and decompression values of the transition pressure. It is possible that local heating may facilitate the transition under these circumstances.⁶⁴

In dynamic shock experiments where maximum pressures are available only for periods of microseconds, phase transitions are found to occur, and in a period of time less than the duration of the shock. This is in marked contrast to experience with static pressures where a sample can

be compressed to a pressure greater than the known thermodynamic pressure and yet give no indication of transformation. Since there is local adiabatic heating during the shock wave it is apparent that the increase in temperature has aided the transition. It was thus felt that if a sample under static pressure could be heated momentarily a more accurate determination of the thermodynamic pressure could be made. A metal wire sample in the Bridgman opposed anvil system described earlier makes an ideal system since electrical ohmic heating by a current pulse enables heating the sample momentarily to essentially any desired temperature.

A review by Kaufman⁶⁵ outlines the thermodynamics and results of metal phase equilibria under pressure. It is easiest to understand phase equilibria from the point of view of free energies G . Figure 23a shows the generalized free energy curves at constant T as a function of pressure for phases A and B, A being the stable low pressure phase. P_T is the "true" transition temperature. The diagram indicates the origin of the region of indifference (apart from frictional effects): if the G curves are closer together than an amount $\Delta G \sim RT$ then the two phases may co-exist. It is seen that $P_T \sim 1/2 (P_u + P_l)$ where P_u is the transition pressure on isothermal compression and P_l is the transition pressure on isothermal decompression. Figure 23b is a $G(P = \text{Const.}) - T$ plot which indicates how an increase in temperature can result in a transition to the high pressure B phase.

The method used in this work involved forming the two different phases in intimate contact at the desired temperature. If in such a situation one phase grows at the expense of the other, it is fairly certain that the growing phase is the thermodynamically stable phase at that temperature. The coexistence of the two phases was obtained by pulse



XBL672-952

Fig. 23 Free energy phase diagrams.

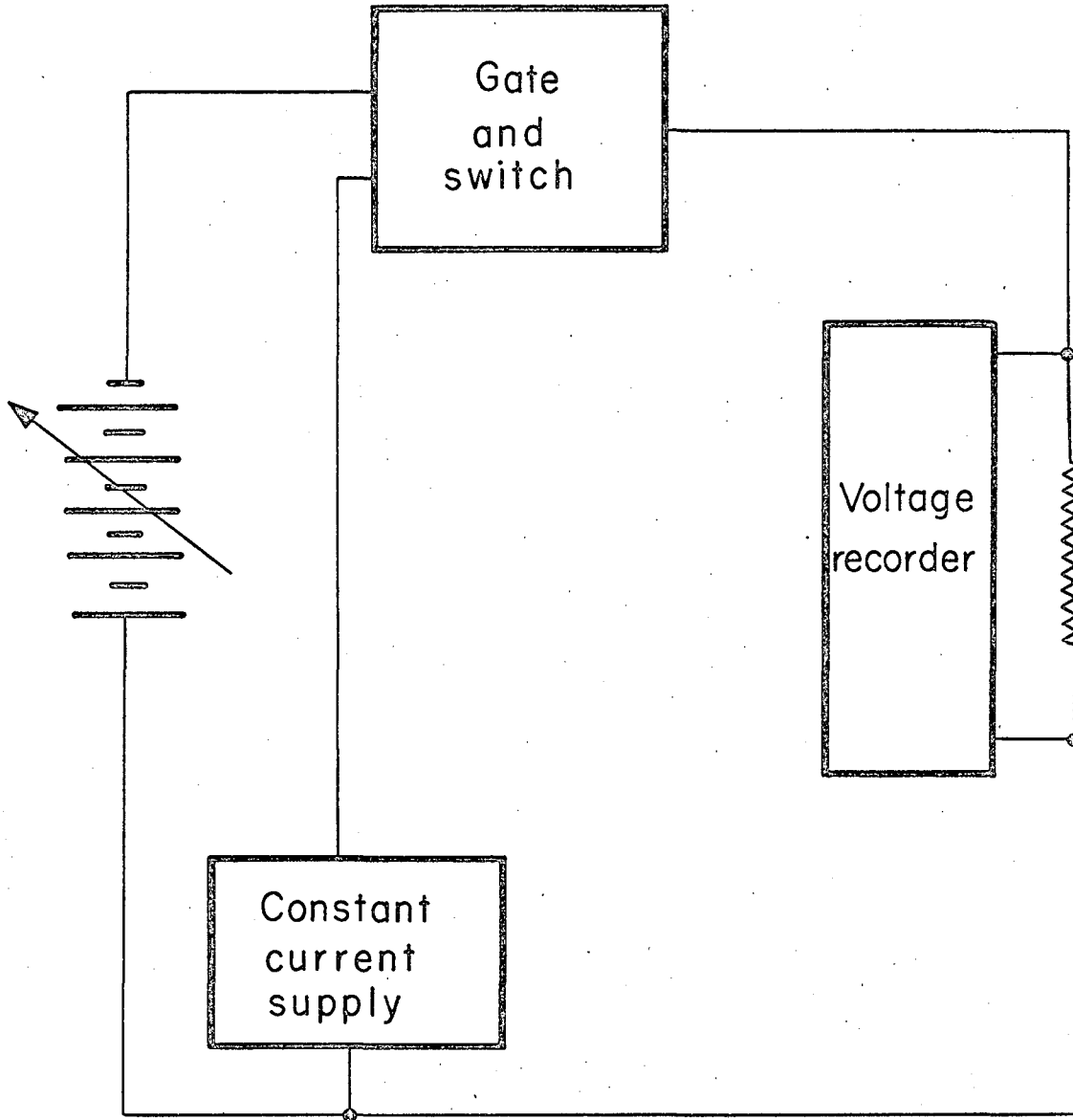
heating; hence it is required that the slope dT/dP of the phase boundary be negative. Conceivably the experiment could also be done by momentarily increasing (or decreasing) the pressure on the sample, but no work has been performed to this end.

One may easily heat a metal sample by passing a high current through it for a short period. For the small ($\sim 10^{-4}$ mole) samples used in this work it was no problem to reach temperatures as high as 1800°K (fixed by the melting of an iron sample). Indeed, the initial problem was one of making the pulse duration short enough that the samples were not melted.

The experimental procedure was somewhat like that described earlier: 0.003" diameter wires were bent into circular arcs and mounted in the Bridgman anvil system. Four lead measurements were not always made; more commonly current was sent into the anvils through Au plugs to the sample and the total voltage drop across the anvils was measured. Fortunately, at room temperature the contact resistances involved are negligible compared to a typical sample resistance of $.2\Omega$ and higher.

The pulsing circuit was simpler than the previously described circuit; a block diagram is shown in Fig. 24. A current source of three 12 volt auto storage batteries connected in parallel was set up so that current could be drawn at voltages of 2-12 volts in 2 volt increments. The outputs of the battery current source and of the constant current supply go to a gating and switching unit which used mechanical mercury reed relays to generate a variable 3-60 millisecond pulse.

Activating the unit shunts current from the constant current supply to a dummy load of 1 ohm after which current from the batteries is directed through the sample. After the preset time of the power pulse, the switching is reversed: the battery current is disconnected and the lower constant



XBL672-953

Fig. 24 Block diagram of simple pulsing circuit.

current is again sent through the sample. The L and N Speedomax recorder monitors the voltage across the sample before and after the high current pulse.

The transition pressure was determined in the following manner: the metal under study is compressed to a pressure 10-20 kbars below the observed isothermal transition pressure. At this point the sample is thermally pulsed, and the resistance followed as a function of time. Proper pulsing changes the resistance of the sample to a value intermediate between the low pressure phase resistance and the high pressure phase resistance. If, after pulsing the resistance returns to its value before the pulse, the pressure is increased by a small amount, the resistance noted, and the sample is pulsed again. If the resistance returns to its initial value, a further pressure increment is made. This procedure is repeated until the resistance remains in the high pressure phase.

The precision of a transformation found in this manner is not as great as when the sample is isothermally compressed in the usual fashion. In the usual experiment, if the transformation starts while the sample is being compressed, the compression can be immediately stopped and the pressure noted. In our technique all that is known is that at some pressure P the material is in one phase, and that after an increment of pressure is added, the material is in another phase. We have assumed that the transition pressure is given by the arithmetic mean between these two pressures.

Several preliminary experiments are needed to determine the optimum conditions to be used. Obviously, the voltage and duration of the heating pulse must have values such that the sample is heated to a sufficiently high temperature, but not so high as to melt the sample. A sufficiently

high temperature is one in which the two phases coexist. In the case of bismuth, the resistance-pressure relation is followed during decompression; if the transition pressure is the same on compression and decompression, the run is discarded as this would indicate that too large an energy pulse was applied, driving the entire sample irreversibly into the high pressure phase. In general, if the pulse strength is such that the entire sample is not transformed to the high pressure form, this difficulty is not encountered.

The geometry of the system is too complex to compute the sample temperature behavior as the energy is electrically generated in the wire. An analysis of a simple and idealized system indicates that the heat leakage from the sample becomes appreciable in tens of microseconds. That this is so can be shown by the fact that a 0.010-sec, 1-volt pulse through a silver sample should melt the entire sample if there were no heat leak. Experimentally it is found that a pulse of about 10 volts is necessary to melt a part of the sample. What has been repeatedly observed is that for a pulse of duration up to 0.060 sec, the temperature of the system, as determined by the resistance of the sample, returns to the ambient temperature in less than 1 min, provided the pressure is far from a transition pressure. The total heat generated is small compared to the heat capacity of the surroundings and the heat leak is large; consequently the short pulse of energy used in these experiments does not appear to have a long-term effect on the temperature of the system. Even though the heat leak from the sample is great, if the duration of the pulse is sufficiently short, the surrounding silver chloride is not appreciably heated, and the sample returns to the ambient temperature in about ten milliseconds after the cessation of electrical heating. If the silver chloride is heated, then a time as long as a minute is required for the

return to room temperature. Either of the foregoing times is short compared to the duration of the study of the effect of the energy pulse. The above can be nicely illustrated with a material such as tin or silver as long as the pressure is far from the transition pressure. If a silver wire 0.003 in. dia and about 1 in. long is pulsed with 6 volts for about 10 millisecc, the resistance returns to its initial value in less than 0.1 min.

The geometry used most commonly in this work was the 1/2" dia. x 3/32" wall x .020" system described in the section on heat capacity. In some cases, notably bismuth, geometries using 1/16" and 1/32" width wall rings were examined. No significant differences were observed. All pressure calibration was based on earlier work in this laboratory.⁴⁴

Results

Bismuth. The bismuth used in these experiments had a supposed purity of 99.999 percent and was supplied by the American Smelting and Refining Company, South Plainfield, New Jersey. It was drawn to wire 0.003 in. dia. The samples were bent into circular arcs of 0.2 in. dia and had resistance of about 2 ohms. Three different geometries were used. It was found that the transition pressure was 81 ± 4 kbars. Conventional isothermal experiments give 88 kbars for the VI-VIII transition. Since the time this work was performed, private communications⁶⁶ have indicated that other experimenters are reproducing the 81 kbar results, both by a pulsing technique, and in the more nearly hydrostatic conditions which prevail in tetrahedral and cubic presses.

Tin. The tin metal was obtained from A. D. MacKay, New York, New York, and was 99.9 percent pure. The metal was extruded to wire 0.003 in. dia and the measurements were made as for bismuth.

The value obtained for the tin transition was 99 ± 4 kbars. This is to be compared to the 107 kbars of Stromberg and Stephens,⁶⁷ and the 113-115 kb reported by Drickamer and Balchan.⁶⁸

Iron. Iron wire, 0.003 in. dia and 99.9 percent pure was obtained from United Mineral and Chemical Company, New York, New York. The work on iron is not as simple or as clearly cut as with the other metals discussed. This situation might be expected from the isothermal work that has been done. Past experience with iron has been that the transition to the hexagonal phase would start at any pressure above 160 kbars and that it might take as much as 80 kbars for the transition to run. This extreme sluggishness could be caused by a small difference in the free energy of the two phases over a wide region of pressure. This argument is supported by the fact that the energy difference between α -iron and γ -iron is small (ΔF of the order 1 kcal/mole⁶⁰). One would not expect a large difference between the γ and hcp-phases; therefore, it seems reasonable that the difference between α -iron and hcp-iron would be small. Since our samples are under quasi-hydrostatic conditions, there is little stress gradient in the sample to aid in the nucleation. Once a pressure of about 80 kbars was reached, there apparently was always a certain amount of sample that transformed to the hexagonal phase. The criterion that was used was that if the resistance decayed with time, then the pressure was below the true transition pressure. It was not feasible to wait for the resistance of the sample to stabilize before going to the next pressure increment as the resistance would decrease for periods longer than one hour. The transition pressure was taken to be that at which no decay occurred in a period of minutes. A total of 21 determinations were made with the voltage of the heating pulse varying from 6 to 12 volts. No dependence on the voltage of the pulse was found.

The transition pressure found for iron is 118 ± 6 kbars; this is again lower than the 130 kbars reported by Drickamer and Balchan,⁶⁸ the ~150 kb found by Fuller and Price,⁶⁹ and the 131 kb derived from the dynamic shock experiments.¹² When the last data are corrected for the shear strength of the metal, a value of ~125 kb is obtained for the transition pressure at the 310°K temperature at which the experiment was run.

Conclusions

To summarize, this thermal pulsing technique was used to investigate the high pressure phase transitions of Bi, Sn, and Fe, obtaining the transition pressures 81 ± 4 kbar, 99 ± 4 kbars and 118 ± 6 kbars, respectively. As would be expected, all three values are lower than the isothermal values obtained in the usual fashion; in the case of iron, good agreement was found with the shock work, where one would expect the associated adiabatic heating to facilitate the transition.

Tin exhibited the sharpest transitions; iron is not as simple as bismuth, but there can be little doubt that a reasonably reproducible value is obtained.

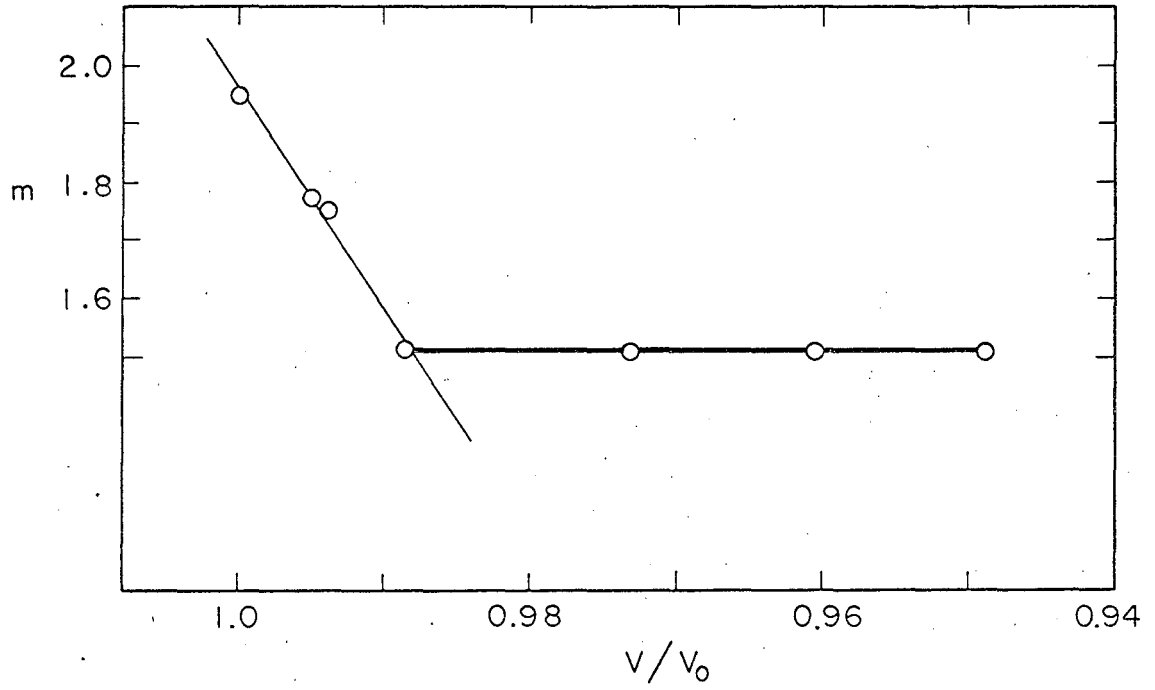
Of the three metals studied, there was no indication that the high-pressure phase was quenched into the system at a low pressure when tin and bismuth were the samples. In the case of iron, a certain amount of the higher pressure phase was present above 80 kb. Time was not taken to determine whether or not the sample would decay completely back to the α phase. The rate at which the hcp-phase decayed was so slow that it was not practical to wait the estimated days from the initial rates for the sample to return to the α form. The fact that part of the sample was in two different phases did not seem to interfere with the determination of the pressure at which the entire sample went and remained hcp.

The pressure scale and calibration used in this work was based on an earlier work, and because of the reproducibility factor involved, the above transition pressures could be used as scale calibration points.

APPENDIX I

As mentioned earlier in this paper, some rather interesting results concerning the temperature dependence of the electrical resistance of iron were observed at pressures greater than 20 kb. Specifically, it appears that at these pressures the electrical resistance of iron is proportional to $T^{3/2}$, T being the absolute temperature, over the temperature range $150^\circ < T < 300^\circ \text{K}$. Several runs at 37 kb indicated that this dependence held down to 77°K . Preliminary experiments on the resistance of cobalt at 50 kb in the temperature interval $200^\circ - 300^\circ \text{K}$ seem to indicate that for cobalt too there is a $3/2$ power law. The experimental results for iron are shown in Fig. 25, in which the exponent m of the power law $R(T)/R(200) = a + bT^m$ has been plotted as a function of reduced volume V/V_0 , where V_0 is the molar volume at atmospheric pressure. It can be seen that m decreases linearly with the volume down to $V/V_0 = .988$, the volume at room temperature and 20 kb; from that point m remains constant at 1.51 down to volumes corresponding to a pressure of 100 kb. The compressibility data collected in Appendix II allowed conversion from pressure to volume, and the exponent for $V/V_0 = 1$ was found from a fit of the data of White and Woods.⁵⁷

Electric current in a metal is carried by electrons whose wave functions extend over the entire lattice; the electrical resistance arises from the scattering of these electrons by various irregularities in the solid. Impurities represent one kind of scattering irregularity, and the thermal vibrations of the ion cores about their ideal lattice points represent another. For pure simple metals ("simple" for the moment meaning having one essentially free valence electron/atom and no d electron complications) it is found that the resistance may be described adequately



XBL673-2262

Fig. 25 Exponent \bar{m} of power law $R(T)/R(200) = a+bT^{\bar{m}}$ for iron as a function of reduced volume.

in terms of electron-phonon interactions; the electrons are scattered by lattice waves. For this scattering, one finds that the resistance is proportional to T for $T \geq \theta_D$, and to T^5 at much lower temperatures ($< \theta_D/10$).

Transition metals with uncompleted d shells prove to have resistances which are quite different from the resistance described above. For instance, if one examines the conductivity per unit amplitude of thermal oscillation, it is found⁷⁰ that the transition metals all have values lower than simple metals by a factor of 10-20. Scattering by lattice waves assumes a resistance proportional to the mean square amplitude of the thermal vibration about the lattice site, which in a Debye approximation means

$$R \propto T/M \theta_D^2$$

If one were to change θ_D by decreasing the volume, one would expect the resistance to change as

$$\left(\frac{\partial \ln R}{\partial \ln V} \right)_T = -2 \left(\frac{\partial \ln \theta_D}{\partial \ln V} \right)_T = 2\gamma$$

where γ is the Grüneisen constant. Now in fact, if $\ln R$ is plotted versus $\ln V$ for iron, the initial slope is found to be 4.7, as compared with 3.4 calculated from the data of Geschneidner.³⁸ The discrepancy indicates that the lattice resistance is only one component of the total resistance.

Discrepancies of this sort resulted in theories⁷⁰ of resistance which attributed a greater scattering probability for those metals having d bands into which the conduction electrons could make transitions. The current is carried by the s electrons, but because of the high density of states in the d band, the probability of transition from an s state to a d state is large, resulting in a larger resistance. The temperature dependence of this

electron-electron resistance varies from T^3 to exponential and depends on the extent of the s and d band overlap.^{25,71,72} Experimentally it is found that at low temperatures, below perhaps 10°K , there is quadratic dependence of the resistance on temperature for iron, cobalt, nickel, platinum, and palladium. At higher temperatures it is known that the resistance increases faster than linearly with the temperature.

Ferromagnetism introduces further complications due to the alignment of the d electron spins; because of the Pauli exclusion principle this alignment effectively limits scattering to unfilled d states from s states having the same spin. The presence of the magnetic domain structure will also affect the resistivity, both because different domains may have different d spin orientations, and because the domain boundaries may additionally scatter the electrons when the mean free path of the conduction electrons becomes comparable to the domain dimensions. The latter effect has been investigated by Semenenko and Sudovtsov.⁷³

The electrical resistance of ferromagnets has been resolved into components by Weiss and Marotta,⁷⁴ who separated the magnetic resistivity by subtracting the residual resistivity and a lattice contribution linear in the temperature from the total measured resistivity. They obtained a spin dependent magnetic resistivity which for iron was about one-quarter of the total resistivity at 300°K and increased approximately quadratically with temperature up to the Curie temperature, 1043°K . At that point the magnetic resistance became constant. These authors point out the dependence of the magnetic resistivity on the spin S of the metal in question; their conclusions agree qualitatively with the theoretical work of Kasuya.⁷⁵ Kaufman and Clougherty^{76,56} have made a similar separation for the resistivity of iron under pressures of up to 95 kb and over a temperature range from 325°K to 1425°K .

Among the various theoretical and experimental work done on the low temperature resistivity of ferromagnets,⁷⁷ the most pertinent to the present work is that of Kondorsky, Galkina and Tchernikova,⁷⁸ Semenko and Sudovtsov,⁷⁹ and Turov.⁸⁰ Kondorsky and co-workers found that the electrical resistance of iron and nickel was proportional to $T^{3/2}$ in the range $4^\circ < T < 20^\circ\text{K}$; Semenko and Sudovtsov found essentially the same result for the interval $1.2^\circ < T < 4.3^\circ\text{K}$ on a purer sample. These investigating groups both attributed this resistance component as resulting from electrons being scattered by spin waves or ferromagnons. The Kondorsky team cites experimental data on the change of resistivity with increasing magnetization as support for this claim.

Turov has carried out a theoretical study of spin wave scattering of electrons and predicts an essentially linear dependence on temperature. However, calculated magnitudes are about three orders of magnitude too small. Turov admits that one might expect a resistivity component proportional to $T^{3/2}$ but that this dependence may be approximated by the function $a_1T + a_2T^2$, the form often observed experimentally. In collaboration with Abel'skii⁸¹ he makes a similar comment on the assumption of a direct proportionality between the resistivity and the density of spin waves.

A simple calculation now leads one to suspect that the resistance temperature relations found here for iron under pressure might be related to spin wave scattering. Using the thermal expansion data of Nix and McNair,⁶¹ one may calculate for iron the change in volume ΔV on going from 300°K to 15°K , the temperature at which the $T^{3/2}$ dependence is observed at zero pressure. By means of the compressibility data of Appendix II, one may find the pressure corresponding to ΔV at room temperature. That pressure is approximately 18 kb, remarkably close to the 20 kb at which the $T^{3/2}$ behavior is first observed.

This tantalizing information however must be approached with caution. The work by the Russian investigators was carried out at temperatures where the resistance due to interaction with lattice waves is very small, whereas in the present investigation this is not the case. If, as Weiss and Marotta, one separates a lattice interaction resistance which is linearly dependent on the temperature, and calculates the changes with pressure of the linear term in the Grüneisen approximation, it is found that at room temperature the lattice contribution is 73% of the total resistance at zero pressure; at 100 kb the lattice contribution has increased to 84% of the total. In that same interval the absolute lattice resistivity has decreased by about 2%. Thus, if indeed for iron it is even meaningful to speak of a (linear) lattice contribution to the total resistivity, it is evident first that the lattice resistivity is the major component of the total resistivity at pressures up to 100 kb and therefore an overall $T^{3/2}$ dependence is due to a strong $T^{1/2}$ dependence superimposed on the linear term. If the lattice resistivity is other than linear then the superimposed function will be different. Secondly, it is obvious that the spin resistivity is decreasing with pressure faster than the lattice resistivity, an observation which somewhat contradicts the data of Kaufman and Clougherty,^{56, 76} who obtain approximately equal relative decreases with pressure for the two resistivity components. Their data however, were taken at temperatures higher than the interval of this work.

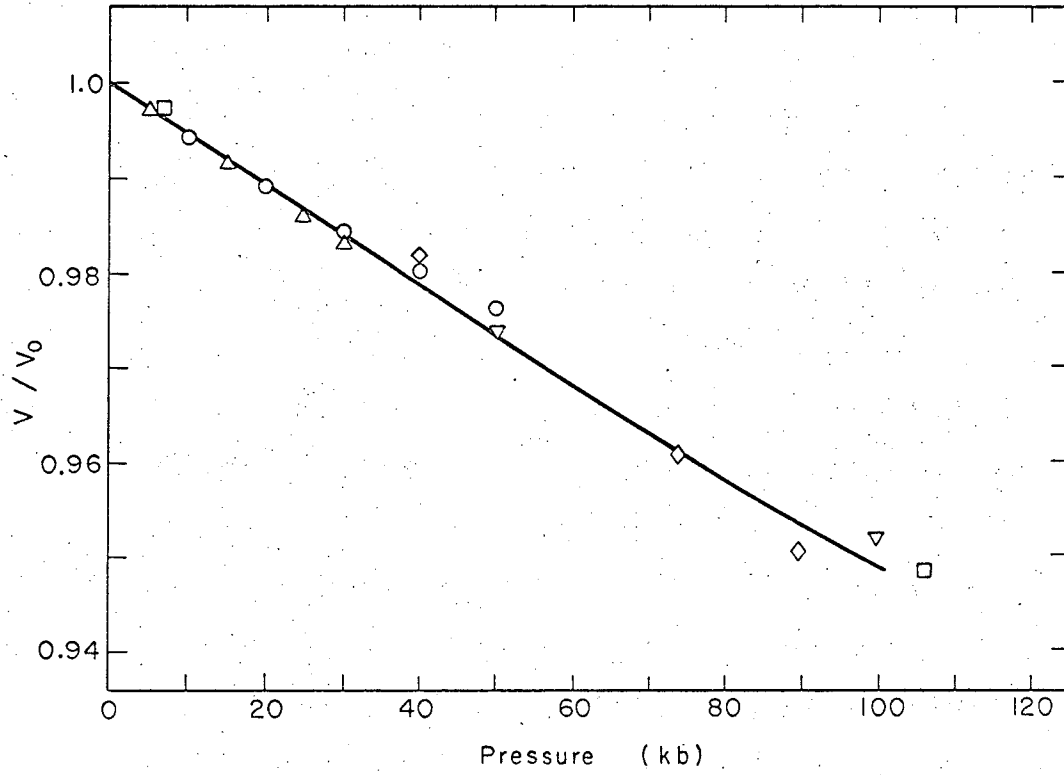
We thus have a resistance phenomenon which most likely reflects changes in the so-called spin resistivity component of the total resistivity. The $T^{3/2}$ temperature dependence of the resistivity at pressures greater than 20 kb suggests that there is an appreciable component due possibly to electron-magnon scattering; it is however somewhat difficult to reconcile this conclusion with the fact that in the temperature range of this work

investigation the lattice contribution to the resistivity is a large fraction of the total, and should not change drastically with pressure. It has also been suggested^{81a} that the range of spin wave \vec{q} vectors available for scattering has a large influence on the temperature dependence of the resistance; a large range could lead to a $T^{3/2}$ relation. Clearly additional study is required. The temperature interval should be increased as much as possible, and research on the effects of impurities, work hardening, surface-to-volume ratios, and domain structure and mobility should be carried out. AC resistance measurements may throw some light on the problem. Several non-magnetic transition metals should be studied as well as the various ferromagnets to investigate an effect which is most likely due to the presence of \underline{d} electrons, but which may only appear in those metals in which the \underline{d} electrons are coupled by some exchange mechanism. To date, vanadium, a face centered cubic structure having 3 \underline{d} electrons per atom has been examined to 130 kb; the temperature dependence of the resistance shows little change from the atmospheric pressure linear behavior.

APPENDIX II

Compression of Iron

The data on the compressibility of iron to 100 kb has been collected and fitted by a least squares method to give the compression graph of V/V_0 versus pressure shown in Fig. 26. Included are the piston displacement data of Bridgman⁸² (○, △), the x-ray diffraction data of Clendenen and Drickamer⁸³ (▽), and of Takahashi and Bassett⁸⁴ (◇), and the corrected shock wave data of Bancroft, Peterson, and Minshall¹² (□). All data except the shock work was carried out at room temperature; the shock wave experiments were performed at slightly lower ambient temperatures (about 283°K). However, the authors of the shock work point out that the temperature rise associated with the adiabatic compression was as high as 27°K at shock pressures of 130 kb; thus the lower pressure shock data is probably in the neighborhood of 300°K. It should also be noted that the shock wave results are for Armco iron while the other investigations were on more pure iron samples.



XBL673-2261

Fig. 26 Compression of iron

APPENDIX III

Experimental Data

In the iron heat capacity work, the results quoted in the main body of the thesis were calculated using graphically smoothed data. In this appendix are presented representative experimental data for 20, 50, and 100 kb isobars. The data are given in tabular form; the reduced resistance $R(T)/R(200)$ and the reduced slope $S(T)/S(200)$ are given at temperatures T . (It will be recalled that S is the slope of the dE/dt versus I^3 linear plot. The heat capacity C is given by the equation $C = RR'/S$, where R' is the temperature derivative of the resistance.)

TABLE I. Experimental Data for 20 kb Isobars

Temperature, °K	$\frac{R(T)}{R(200)}$	$\frac{S(T)}{S(200)}$
149.2	.629	.557
155.8	.672	.666
162.1	.718	.718
169.0	.770	.744
176.7	.828	.783
183.8	.877	.856
190.8	.929	.948
198.1	.984	1.014
207.7	1.059	1.062
215.2	1.115	1.129
223.6	1.183	1.156
230.6	1.238	1.250
241.4	1.327	1.294
248.8	1.391	1.439
148.7	.624	.627
151.4	.639	.600
159.0	.695	.677
164.2	.732	.729
170.6	.778	.781
182.2	.864	.809
187.8	.906	.888
194.5	.957	.943
201.7	1.011	1.019
207.2	1.056	1.073
213.3	1.102	1.074
219.7	1.151	1.198
225.5	1.199	1.221
230.6	1.233	1.255
236.9	1.290	1.367
243.0	1.339	1.391
248.5	1.385	1.410
254.5	1.434	1.505
260.9	1.488	1.465
266.9	1.537	1.640
272.7	1.589	1.644
278.6	1.636	1.663
283.1	1.677	1.920

TABLE II. Experimental Data for 50 kb Isobars

Temperature, °K	$\frac{R(T)}{R(200)}$	$\frac{S(T)}{S(200)}$
146.4	.605	.636
152.7	.644	.650
158.5	.691	.680
164.8	.734	.725
171.2	.780	.779
177.3	.826	.798
183.5	.873	.901
189.4	.918	.936
194.9	.961	.966
201.2	1.010	1.007
207.5	1.056	1.067
213.2	1.102	1.099
219.1	1.150	1.155
225.8	1.203	1.207
231.9	1.252	1.246
238.2	1.303	1.321
243.8	1.351	1.358
250.0	1.402	1.407
256.6	1.458	1.536
264.1	1.518	1.481
270.7	1.578	1.565
277.2	1.634	1.709
150.0	.631	.626
155.5	.669	.685
161.6	.713	.717
182.2	.863	.884
189.2	.917	.936
196.5	.973	.931
203.2	1.025	.997
210.5	1.080	1.122
225.6	1.200	1.174
233.2	1.260	1.268
255.1	1.441	1.411
263.1	1.507	1.488
148.0	.613	.624
156.2	.670	.705
162.6	.720	.723
170.0	.769	.795
176.7	.825	.850
183.8	.881	.916
192.5	.944	.959
201.2	1.006	1.054
208.1	1.058	1.086

TABLE II (Continued)

Temperature, °K	$\frac{R(T)}{R(200)}$	$\frac{S(T)}{S(200)}$
215.2	1.114	1.139
222.8	1.177	1.210
230.0	1.233	1.228
237.2	1.293	1.306
244.0	1.346	1.400
251.2	1.405	1.413
259.0	1.470	1.539
265.8	1.527	1.600
272.7	1.585	1.758
279.8	1.649	1.770
296.1	1.803	2.078

TABLE III. Experimental Data for 100 kb Isobars

Temperature, °K	$\frac{R(T)}{R(200)}$	$\frac{S(T)}{S(200)}$
147.1	.606	.633
153.9	.655	.671
161.1	.706	.730
168.4	.759	.774
175.4	.813	.797
183.4	.871	.889
190.4	.925	.965
198.0	.984	.950
205.2	1.040	1.037
212.0	1.093	1.062
219.4	1.153	1.175
226.7	1.211	1.210
233.7	1.268	1.283
240.9	1.326	1.392
248.3	1.388	1.434
254.9	1.442	1.489
261.9	1.503	1.486
268.5	1.560	1.570
276.8	1.630	1.608
283.9	1.693	1.796
295.1	1.796	1.898
146.7	.601	.611
154.5	.655	.652
161.9	.711	.748
169.4	.766	.750
176.5	.818	.803
184.5	.878	.877
191.2	.930	.950
198.0	.981	1.032
204.3	1.032	1.049
211.6	1.102	1.109
218.9	1.149	1.167
226.3	1.207	1.266
234.2	1.272	1.339
240.9	1.326	1.351
248.2	1.387	1.352
254.9	1.445	1.482
261.5	1.501	1.506
275.8	1.625	1.730
282.3	1.685	1.786
287.0	1.724	1.892
295.4	1.802	2.004

ACKNOWLEDGMENTS

I would like to express my very sincere thanks to Dr. George Jura, whose insight, inspiration, and guidance were a continual aid during the course of this work.

I also owe many thanks to members of the high pressure group here, including Mr. Duane Newhart, who gave generously of his able technical and mechanical assistance, and my co-workers Dr. Donald Raimondi, Mr. John Przybylinski, and Mr. James Burton, who contributed a great deal through discussion and assistance.

Finally, a word of thanks must go to the many individuals and divisions of the Lawrence Radiation Laboratory, Berkeley, who contributed their skills and knowledge to many separate aspects of this project.

This work was performed under the auspices of the United States Atomic Energy Commission.

REFERENCES

1. P. W. Bridgman, *Rev. Mod. Phys.*, 18, 1 (1946).
2. S. A. Zlunitzin, *Zhur. Eksptl. i Teoret. Fiz.*, 9, 72 (1939).
3. O. N. Trapeznikov and G. A. Milyutin, *Nature*, 144, 632 (1939).
4. P. W. Bridgman, *The Physics of High Pressures*, (G. Bell and Sons, London, 1958).
5. F. J. Webb, K. R. Wilkinson, and J. Wilks, *Proc. Roy. Soc.*, (London), A214, 516 (1952).
6. J. S. Dugdale and F. E. Simon, *Proc. Roy. Soc.* (London), A218, 291 (1953).
7. G. Ahlers, Some Properties of Solid Hydrogen at Small Molar Volumes. (Ph.D. Thesis), UCRL 10757, June 1963.
8. J. C. Ho, N. E. Phillips, and T. F. Smith, *Phys. Rev. Letters*, 17, 694 (1966).
9. J. C. Ho and N. E. Phillips, private communication.
10. D. L. Raimondi, to be published.
11. M. H. Rice, R. G. McQueen, and J. M. Walsh, in *Solid State Physics*, Vol. 6 (Academic Press, New York, 1964).
12. D. Bancroft, E. L. Peterson, and S. Minshall, *J. Appl. Phys.*, 27, 291 (1956).
13. L. V. Al'tshuler, et al., *Soviet Physics JETP*, 34, 606 (1958).
14. G. E. Duvall and G. R. Fowles, in *High Pressure Physics and Chemistry*, Vol. 2, R. S. Bradley, Ed. (Academic Press, London, 1963).
15. R. G. McQueen, in *Metallurgy at High Pressures and High Temperatures*, (Gordon and Breach, New York, 1964).
16. R. V. Pound and G. A. Rebka, *Phys. Rev. Letters*, 4, 274 (1960).

17. R. S. Preston, S. S. Hanna, and J. Heberle, *Phys. Rev.*, 128, 2207 (1962).
18. M. Nicol and G. Jura, *Science*, 141, 1035 (1963).
19. D. Phillips, *The Magnetic and Electrical Properties of Some Metals at High Pressures* (Ph.D. Thesis), UCRL-16299, August 1965.
20. D. N. Pipkorn, et al., *Phys. Rev.*, 135, A1604 (1964).
21. D. L. Raimondi, *Effect of High Pressure on the Properties of Some Metals* (Ph.D. Thesis), UCRL-17095, Sept. 1966.
22. V. N. Panyushkin and F. F. Voronov, *JETP Letters*, 2, 97 (1965).
23. D. C. Wallace, P. H. Sidles, and G. C. Danielson, *J. Appl. Phys.*, 31, 168 (1960).
24. C. Kittel, Introduction to Solid State Physics, 3rd. Edition (John Wiley and Sons, New York, 1966).
25. J. M. Ziman, Electrons and Phonons, (Oxford University Press, Oxford, 1963).
- 25a. J. M. Ziman, Principles of the Theory of Solids, (Cambridge University Press, Cambridge, 1964).
26. M. Born and K. Huang, Dynamical Theory of Crystal Lattices, (Oxford University Press, Oxford, 1962).
27. J. de Launay, in Solid State Physics, Vol. 2, (Academic Press, New York, 1956).
28. M. Born and T. von Karman, *Physik Z.*, 14, 15 (1913).
29. C. W. Garland and G. Jura, *J. Chem. Phys.*, 22, 1108 (1954).
30. W. Stark and R. N. Kortzeborn, UCRL-17225, Oct. 1966.
31. D. C. Wallace, *Rev. Mod. Phys.*, 37, 57 (1965).
32. E. Grüneisen, in Handbuch der Physik, Vol. 10 (J. Springer, Berlin, 1926).

33. G. Liebfried and W. Ludwig, in Solid State Physics, Vol. 12 (Academic Press, New York, 1961).
34. G. N. Lewis and M. Randall, Thermodynamics, (McGraw-Hill Book Co., New York, 1961).
35. J. J. Burton and G. Jura, private communication.
36. C. H. Hinricks and C. A. Swenson, Phys. Rev., 123, 1106 (1961).
37. J. E. Schirber and C. A. Swenson, Phys. Rev., 123, 1115 (1961).
38. K. Geschneidner, in Solid State Physics, Vol. 16 (Academic Press, New York, 1964).
39. J. A. Hofman, et al., J. Phys. Chem. Solids, 1, 45 (1956).
- 39a. A. B. Pippard, The Elements of Classical Thermodynamics, (University Press, Cambridge, 1964).
40. N. F. Mott and H. Jones, The Theory of the Properties of Metals and Alloys, Chapter 6, (Dover Publications, New York, 1958).
41. L. Patrick, Phys. Rev., 93, 384 (1954).
42. L. B. Robinson, F. Milstein, and A. Jayaraman, Phys. Rev., 134, A187, (1964).
43. D. Bloch and R. Pauthenet, Compt. Rend., 254, 1222 (1962).
44. D. B. McWhan and A. L. Stevens, Phys. Rev., 139, A682 (1965).
45. D. L. Raimondi, Private communication.
46. D. B. McWhan, Private communication.
47. H. S. Carslaw and J. C. Jaeger, Conduction of Heat in Solids, (Oxford University Press, London, 1959).
48. P. W. Montgomery, et al., in High Pressure Measurement (Butterworths, Washington, 1962).
49. H. Stromberg and G. Jura, Science, 138, 1344 (1962).
50. G. C. Kennedy and P. N. LaMori, in Progress in Very High Pressure Research, (John Wiley and Sons, New York, 1961).

51. P. C. Souers and G. Jura, *Science*, 140, 481 (1963).
52. P. C. Souers, Effect of High Pressure on the Electrical Resistance of Bi, Yb, and Dy (Ph.D. Thesis), UCRL-11220, Jan. 1964.
53. G. Urbain, P. Weiss, and F. Trombe, *Compt. Rend.*, 200, 2132 (1935).
54. H. E. Nigh, S. Legvold, and F. H. Spedding, *Phys. Rev.*, 132, 1092 (1963).
55. M. Griffel, R. E. Skochdopole, and F. H. Spedding, *Phys. Rev.* 93, 657 (1954).
56. L. Kaufman, E. V. Clougherty, and R. J. Weiss, *Acta Met.*, 11, 323 (1963).
57. G. K. White and S. B. Woods, *Phil. Trans. Roy Soc, London*, A251, 273 (1958).
58. Handbook of Chemistry and Physics, (Chemical Rubber Publishing Co., Cleveland, 1956).
59. P. W. Bridgman, *Proc. Am. Acad. Art and Sci.*, 81, 165 (1952).
60. H. Margenau and G. M. Murphy, The Mathematics of Physics and Chemistry (Van Nostrand, New York, 1962).
61. F. C. Nix and D. McNair, *Phys. Rev.* 60, 597 (1941).
62. K. K. Kelley, *J. Chem. Phys.*, 11, 16 (1943).
63. Selected Values for the Thermodynamic Properties of Metals and Alloys, Minerals Research Laboratory, Inst. of Engineering Research, University of California, Berkeley, California.
64. R. E. Harris and G. Jura, in Elemental Sulfur, B. Meyer, Ed., (Interscience, New York, 1965).
65. L. Kaufman, in Solids Under Pressure, W. Paul and D. M. Warschauer, Eds., (McGraw-Hill, New York, 1963).
66. D. R. Stephens, Private communication.

67. H. S. Stromberg and D. R. Stephens, *J. Phys. Chem. Solids*, 25, 1015 (1964).
68. H. G. Drickamer and A. S. Balchan, in Modern Very High Pressure Techniques, (Butterworths, London, 1962).
69. P. J. A. Fuller and J. H. Price, *Nature*, 193, 262 (1962).
70. N. F. Mott and H. Jones, op cit, Chapter VII.
71. D. A. Goodings, *Phys. Rev.*, 132, 542 (1963).
72. A. J. Dekker, *J. Appl. Phys.*, 36, 906 (1965).
73. E. E. Semenenko and A. I. Sudovtsov, *Soviet Physics JETP*, 20, 323 (1965).
74. R. J. Weiss and A. S. Marotta, *J. Phys. Chem. Solids*, 9, 302 (1959).
75. T. Kasuya, *Prog. Theoret. Phys. (Kyoto)*, 16, 58 (1956).
76. E. V. Clougherty and L. Kaufman, in High Pressure Measurement, A. A. Giardini and E. C. Lloyd, Eds. (Butterworths, Washington, 1963).
77. In addition to the papers cited in the text see:
S. V. Vonsovskii, *Bull. Acad Sci USSR Physical Series*, 19, 447 (1955).
Translated by Columbia Technical Translations, 1956.
78. E. Kondorsky, O. S. Galkina, and L. A. Tchernikova, *J. Appl. Phys.*, 29, 243 (1958).
- 78a. E. I. Kondorskii, O. S. Galkina, and L. A. Chernikova, *Soviet Physics JETP*, 34, 741 (1958). This is essentially the same paper as cited in Reference 78.
79. E. E. Semenenko and A. I. Sudovtsov, *Soviet Physics JETP*, 15, 708 (1962).
80. E. A. Turov, *Izv. Akad. Nauk SSSR, Ser. Fiz.*, 19, 474 (1955). Translation by Columbia Technical Translations, 1956.
- 80a. E. A. Turov, *Fiz. metal. metalloved.*, 6, 203 (1958).
81. Sh. Sh. Abel'skii and Ye. A. Turov, *Fiz. metal. metalloved.*, 6, 203 (1958).

- 81a. J. W. Halley, Private communication.
82. P. W. Bridgman, Proc. Am. Acad. Art Sci., 72, 207 (1938).
- 82a. P. W. Bridgman, Proc. Am. Acad. Art Sci., 77, 189 (1949).
83. R. L. Clendenen and H. G. Drickamer, J. Phys. Chem. Solids, 25,
865 (1964).
84. T. Takahashi and W. A. Bassett, Science, 145, 483 (1964).

This report was prepared as an account of Government sponsored work. Neither the United States, nor the Commission, nor any person acting on behalf of the Commission:

- A. Makes any warranty or representation, expressed or implied, with respect to the accuracy, completeness, or usefulness of the information contained in this report, or that the use of any information, apparatus, method, or process disclosed in this report may not infringe privately owned rights; or
- B. Assumes any liabilities with respect to the use of, or for damages resulting from the use of any information, apparatus, method, or process disclosed in this report.

As used in the above, "person acting on behalf of the Commission" includes any employee or contractor of the Commission, or employee of such contractor, to the extent that such employee or contractor of the Commission, or employee of such contractor prepares, disseminates, or provides access to, any information pursuant to his employment or contract with the Commission, or his employment with such contractor.

